

**A MATRIX ISOLATION SPECTROSCOPIC INVESTIGATION INTO THE
REACTION PRODUCTS OF VANADIUM METAL ATOMS WITH PROPENE**

by

Stephen W.C. Walker

A thesis submitted to the Department of Chemistry

In conformity with the requirements for

the degree of Masters of Science

Queen's University

Kingston, Ontario, Canada

August, 2009

Copyright © Stephen William Charles Walker, 2009

Abstract

The products of vanadium metal atom reactions with propene and some propene isotopomers (propene-d₆ and propene-3,3,3-d₃) are investigated using FT-IR matrix isolation. The major product from the condensation of V atoms with propene at elevated mole ratios is found to be propane (C₃H₈), the production of which is seen to increase as concentration of propene increases. Additionally a matrix isolated product formed after metal atom insertion into the C-H bond of propene at low propene mole ratios is isolated and identified.

The location of the insertion site is identified as one of the methyl hydrogen carbon bonds. The structure of the product is identified as an allyl vanadium hydride complex, through a FT-IR matrix isolation study of propene isotopomers. It is also shown that this primary product acts as an intermediate in the formation of propane. A full mechanism for the proposed formation of propane from sacrificial hydrogenation is proposed and compared with the reported mechanism for the similar reaction involving ethene. The mechanistic identification of the hydrogenation of propene is shown as a generalization of the previous reaction involving ethene.

Photochemistry of reactants and intermediates trapped in the matrix are investigated. Irradiation of matrices with several different UV-visible wavelength ranges indicate that no further chemistry occurs after formation of the matrix and further irradiation has no effect on intermediates or reactants. Additionally the reactivity of water with vanadium and propene under low propene concentration

conditions is also studied. Results from this study show that under all conditions studied no incorporation of water into the propene molecule is found.

Acknowledgements

I would like to first thank all of the staff and faculty at both Queen's and Trent Universities specifically those in the chemistry departments of the two institutions, I have benefited greatly from your help and guidance. I have been lucky enough to have studied from several great professors at both institutions.

I would like to thank my supervisor J. Mark Parnis, his help and guidance has made this possible. Without his encouraging words and helpful ideas there is no way I could have done this. He truly encapsulates the meaning of teacher, one of the greatest ones I have been lucky enough to meet let alone work for. Thank you.

I would also like thank the tremendous help that my peers in the Parnis Lab throughout the years. I would like to thank Kaitlynn King, Laura Prest, and Brandi West for their support and friendship. I would like to thank Dr. Matthew Thompson; with out his help this project would not have been possible. The ability to bounce ideas and discuss the project with some one with direct experience was invaluable. Throughout the process of my undergraduate and graduate career in the Parnis lab I have met two of my closest friends Matt White and Adam Malcolm. I never thought that I could have had so much fun working and I know that with out their friendship I could not have achieved this in such good spirits or have learned so much.

I would finally like to thank some of teachers that I have been around the longest, my family. Although with a complete absence of mathematic skills

without my sister Kate there is no way I could have achieved what I have. Her drive and ambition has certainly finally rubbed off. I hope that one day I can write one tenth as well as her.

No other people have taught me so much about thinking, and life or have influenced me more then my parents, Jim and Denise Walker. Thank you for your help, guidance, motivation and above all love. GBC. Respect.

To Mom and Dad

Table of Contents

Abstract	ii
Acknowledgments	iv
Table of Contents	vii
List of Figures and Schemes	ix
List of Tables	xiii
Chapter 1: Introduction	1
1.0 Matrix Isolation.....	2
1.1 Fourier transformed infrared spectroscopy (FTIR) Matrix Isolation.....	7
References for Chapter 1	16
Chapter 2: Literature Review	18
2.0 Brief introduction of transition metal reactivity	18
2.1 Transition metal chemistry with hydrocarbons	19
2.2 Gas phase reactions of transition metals with hydrocarbons.....	20
2.2.0 Cluster Chemistry	20
2.2.1 Transition metal atom reactions with acetylene and other alkynes.....	21
2.2.2 Reactions of metal atoms with ethene and propene	23
2.3 Metal atoms in inert gas matrices	31
2.4 Alkenes in inert gas matrices	36
2.5 Reactions of metal atoms with simple hydrocarbons at low temperatures	37
References for Chapter 2	46
Chapter 3: Experimental.....	49
3.0 Materials	49
3.1 Gas Handling Line	50
3.2 Preparation of Gas Sample	51
3.3 Metal Deposition Matrix Isolation Apparatus.....	54
3.3.1 Vacuum System.....	55
3.3.2 Cooling System.....	55
3.3.3 Gas Handling within the Matrix Isolation Apparatus.....	56
3.4 Reaction Chamber	56

3.4.1	Vaporization of metal atoms	57
3.4.2	Quartz Crystal Microbalance	58
3.4.3	Metal filament preparation	59
3.4.4	Spectral Windows	59
3.5	Irradiation and annealing of matrices.....	60
3.6	Procedure for isotopic substitution work with water	61
	References for Chapter 3	62
 Chapter 4: Results.....		63
4.0	Overview.....	63
4.1	Vanadium reactivity towards propene in argon matrices	64
4.2	Optimization of propane.....	72
4.2.1	Variation of propene concentration	72
4.2.2	Variation of metal flux	75
4.2.3	Variation of gas flow	78
4.3	Reactions of V with isotopes of propene: V+C ₃ D ₆ and C ₃ D ₃ H ₃	81
4.3.1	Reaction of V with C ₃ D ₆	81
4.3.2	Reaction of V with C ₃ D ₃ H ₃	86
4.4	Reaction of V + propene in the presence of water.....	88
4.4.1	Reaction of H ₂ O with C ₃ D ₆ and V	88
4.4.2	Reactions of D ₂ O with C ₃ H ₆ and V.....	92
	References for Chapter 4	94
 Chapter 5: Discussion		95
5.0	Propane production	95
5.0.1	Production of propane- experimental conditions.....	96
5.0.2	Effect of irradiation and comparison with ethene	99
5.0.3	Isotopic substitution of H analysis.....	101
5.1	The additional/intermediate product.....	104
5.1.1	Production of the additional product- experimental conditions.....	104
5.1.2	Structural analysis of infrared results.....	107
5.1.3	Structural analysis – Isotopic study.....	111
5.2	Water work	114
5.3	Formation of propane mechanism	118
	References for Chapter 5	124
 Chapter 7: Summary		125

List of Figures and Schemes

- Figure 1:** Cartoon structure of an argon matrix with different species isolated within. _____ 4
- Figure 2:** Infrared spectra of the C-H stretching region of matrix isolated ethyne (C_2H_2), ethene (C_2H_4), and ethane (C_2H_6) _____ 9
- Figure 3:** Comparison of the SO_2 IR modes both in the gas phase and the matrix isolated _____ 12
- Figure 4:** Comparison of the UV-visible absorptions of V atoms in an Ar matrix and the blackbody emission profile at 3680K _____ 33
- Figure 5:** Gas handling pipeline used for preparation of gas sample _____ 50
- Figure 6:** Schematic diagram of the metal deposition matrix isolation apparatus, the cold tip and expander can be rotated such that it is possible to, deposit, irradiate and acquire a spectrum. _____ 54
- Figure 7:** Schematic diagram of the interior of the reaction chamber used in the metal deposition matrix isolation apparatus the electrodes are cooled with flowing water throughout the deposition. _____ 57
- Figure 8:** Full spectrum of C_3H_6 with and without metal present. 1:100 propene:Ar at 2.5 sccm/min, vanadium was deposited at 3 cpm for the duration of the deposition _____ 65
- Figure 9:** A difference spectrum of the reference spectrum subtracted from the deposition with 3 cpm of vanadium. _____ 66

Figure 10: Irradiation at several different wavelengths of light shows very little change. _____	67
Figure 11: Comparison of matrix isolated and the difference spectrum obtained by subtraction of the reference from the deposit with vanadium. _____	69
Figure 12: The normalized areas of several propane features from subtraction spectra are plotted against the mol fraction of propene to argon. _____	73
Figure 13: The areas of several non propane features from subtraction spectra are plotted against the mol fraction of propene to argon. _____	74
Figure 14: Selection of the infrared spectrum for 1:100 propene:Ar displaying the key regions for some of the propane features at three different metal flows ____	76
Figure 15: Selection of the infrared spectrum for 1:1000 propene:Ar displaying the key regions of the non-propane features at three different metal flows ____	77
Figure 16: Portion of the resulting difference spectrum of the deposition of 1:100 C ₃ D ₆ . _____	82
Figure 17: Comparison of the C-H stretching region (left of break) and the C-D stretching region along with majority of the rest of the spectrum (right of break) for the resulting difference spectrum of 1:100 propene-d ₆ after deposition with 3 cpm of vanadium. _____	89

Figure 18: Comparison of the C-H stretching region (left of break) and the C-D stretching region along with majority of the rest of the spectrum (right of break) for the resulting difference spectrum of 1:1000 propene-d ₆ after deposition with 3 cpm of vanadium_____	90
Figure 19: Comparison of the C-H stretching region (left of break) and the C-D stretching region along with majority of the rest of the spectrum (right of break) for the resulting difference spectrum of 1:400 propene-d ₆ after deposition with 7 cpm of vanadium. _____	91
Figure 20: C-H and C-D stretching regions (left of break) and portions of the rest of the resulting difference spectrum after 1:100 propene:Ar with 1 torr D ₂ O deposited with 3-5 cpm V. _____	93
Figure 21: The two possible structures for the intermediate product based on their infrared absorptions. _____	108
Scheme 1: Intermediate complexes mechanisms A) the allyl product and B) the methylacetylene product_____	110
Scheme 2: The mechanisms illustrating the formation of the two possible structures for the primary product using propene-3,3,3-d ₃ . _____	112
Scheme 3: Reaction mechanism for production of propane from propene hydrogenation with vanadium metal atoms_____	119

Figure 22: Structural representation of the possible reaction mechanism for the formation of propane from propene hydrogenation with vanadium metal atoms.

120

List of Tables

Table 1: Wavenumber positions of new features in the resulting spectrum along with features that show a decrease in intensity following the reaction of V + 1:100 C ₃ H ₆ :Ar.	70
Table 2: Wavenumber positions for the features following the reaction of V + 1:100 C ₃ H ₆ :Ar other than those corresponding to propane.	70
Table 3: The areas of several features that appear on deposition with V under several different flow rates (1:1000)	79
Table 4: The areas of several features that appear on deposition with V under several different flow rates (1:200)	79
Table 5: Wavenumber positions for the various products observed in the infrared spectra following reaction of V +1:100 C ₃ D ₆ :Ar.	83
Table 6: Wavenumber positions for the unidentified product observed in the infrared spectra following reaction of V +1:100 C ₃ D ₆ :Ar	85
Table 7: Wavenumber positions of observed features after deposition of several different concentrations of C ₃ D ₃ H ₃ with V	87
Table 8: Positions of new bands of a metal containing species on deposition of propene with metal, with possible assignments for two suspected intermediate structures	109

Chapter 1

Introduction

Hydrocarbons are among the most ubiquitous chemical compounds. From synthetic chemistry to the petrochemical and pharmaceutical industries, they are used due to their relative abundance and chemical versatility.¹ While the strong CH bond of hydrocarbons contributes to the stability of the resulting products, it also leads to difficulty in their use as starting materials for chemical synthesis. Thus any chemical process which increases the reactivity of the CH bond is a widely useful and sought-after approach. Carbon-hydrogen bond activation by metal atom insertion is one method that can be used in many cases.

The present work is an attempt to gain a more comprehensive understanding of the nature of these metal-hydrocarbon interactions. Specifically, reactions of vanadium and propene are studied in detail. Past research has shown transition metal atoms to have both the ability to coordinate with many monomers of ethene evolving H₂,² as well as to participate in a dehydrogenation-hydrogenation mechanism leading to ethane.³ The hydrogen molecule elimination work was conducted in the gas phase and only resulted in information of the product mass. It did not go into an explanation of the mechanism for this process. The work done by Thompson et al. was an effort to illuminate this mechanism using a FT-IR matrix isolation process identical to the one employed in the present work. The aim of the present study was to explore the mechanism proposed in reference 3 with propene to see if it can be

generalized to other hydrocarbons and to get a better understanding of the mechanism. Propene is the next simplest hydrocarbon after ethene and can be thought of as 1-methyl ethene. As vanadium was used for the majority of the previous studies with ethene, it was used again here.

To gain mechanistic information about any possible reaction of propene with V, structural information of intermediates along with reactants and products is needed in order to infer a possible reaction pathway. Matrix isolation Fourier Transform Infrared Spectroscopy, (FT-IR MI) provided the main method for analysis of the reaction in the study.

1.0 Matrix Isolation

Originally designed as an instrumental technique for gaining spectroscopic information of gas phase molecules in the 1950's by Pimentel⁴ rare gas matrix isolation has since shown to be a powerful method for determining mechanistic data for transient species.⁵ A sample of the molecule to be studied (known as the sample gas) is surrounded by a much higher concentration of an "inert" host gas also known as the matrix gas. The host gas is frozen on a spectroscopic window held below the freezing point of the host gas. The host gas then forms a solid structure known as the matrix, in which the sample gas is trapped. As the concentration of host gas is much higher than the sample gas (1000:1 and higher for full isolation) the molecules of the sample gas are fully separated from one another. In order to give the most accurate representation of the pure sample gas

the matrix gas must be inert with respect to interaction with the sample gas and be spectroscopically invisible with the type of irradiation used to analyze the sample gas in the range used. Several gases have been used as matrix materials depending on the specific properties needed for the given experiment. Gases that can more effectively absorb energy such as nitrogen and methane have been included as the matrix material. This will help to lower the vibrational energy of excited hot gas molecules during condensation.⁶ Argon has become the gas of choice for many situations where collisional deactivation is not quite as important, as argon has many properties that seem to be perfect for matrix isolation. The electronic configuration of argon $[\text{Ne}]3s^23p^6$ having a full outer shell of electrons leads to its inertness with respect to reactivity and it is known to be a very non-reactive gas. As an atomic gas it has no molecular structure, and as such it does not have any vibrational modes, causing it to be invisible in the infrared (IR) range of the electromagnetic spectrum. This enables it to be used for matrix isolation when the identification technique used is IR spectroscopy. The freezing point of argon at 83.8K allows it to gain a rigid structure when cooled using a helium condenser, which is the main cooling technique used in matrix isolation. Finally, argon makes up about 1% of the earth's atmosphere; it is the 3rd most abundant component in dry air after nitrogen and oxygen⁷ and is a byproduct of the separation of air in the production of purified nitrogen. This lowers the cost of argon compared to other relatively rarer non-reactive gases used for matrix isolation.

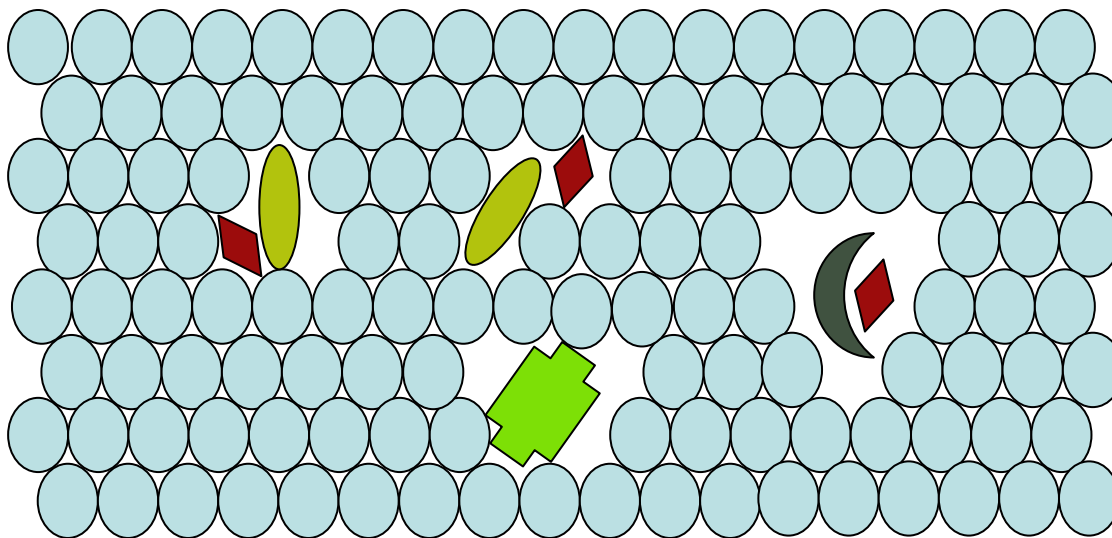


Figure 1: Cartoon structure of an argon matrix with different species isolated within.

Matrix isolation enables the mechanistic study of gas phase molecules by trapping not only products of the reaction, but any possible intermediates along the way. Identifying the structure of the intermediates is key in understanding the mechanism as they can be considered snap shots of the reaction along its path. The low temperature of the matrix (13-20K) causes structures to become stabilized in energy minima even if the energy barrier to further reaction of isomerization is low, since there is so little internal energy available to overcome these states. At the temperatures used in rare gas matrix isolation the internal energy is quite low and can be calculated from $(3/2)kT$ for a unimolecular process and $3kT$ for a bimolecular process. This gives a energy of about 160 J/mol available for a unimolecular process at 13K.

While this does stop most reactions happening once the matrix has fully formed, some reactions such as radical-radical recombination reactions are barrierless and would occur in a matrix if they were isolated together. However the argon acts like a cage once it is formed. This helps to inhibit further reaction of the sample gas and limits any possibility of bimolecular reactions. While the argon traps the sample species, its low reactivity is imperative as it allows for the simulation of the traditional gas phase chemistry that is being studied. The more the sample can interact with a given host gas the less it can be used as an experimental homolog for the original reaction.

Control over the reaction is another aspect that is needed for mechanistic identification. By being able to control the completeness of a reaction and the direction a reaction goes, one is able to study the key aspects of a given reaction without clutter from other side reactions that may be occurring. Controlling the reaction in the case of this work is done by the ability to vary key conditions in the reaction; gas flow, metal flow, and the concentration of sample gas. Varying the gas flow controls three aspects of the reaction: first, increase in gas flow causes a higher pressure within the reaction zone before the matrix is fully formed. Higher pressure can alter the apparent chemistry by increasing the total amount of possible collisions per unit of time. Second, it can control for the concentration of metal atoms captured in the matrix, since at higher flow there is more matrix material per metal atom than at low flow. Thirdly, with more material forming the matrix, the temperature will rise due to thermal load. This increase in temperature may increase diffusion throughout the matrix, increasing the likelihood of further

reactions occurring. Metal flow variation again controls the concentration of metal found in the matrix. It also controls the formation of metal dimers, which can show much different chemistry to that of single metal atoms.⁸ Increasing the metal flow increases the likelihood of having a metal atom and reactive species coming in contact with the correct orientation and energy such that they can react. Varying the concentration of sample to host gas controls the reaction pathway. Higher concentrations promote the likelihood of multiple sample species coming in contact with a metal atom before freezing, which can lead to interesting reactions between multiple molecules of the sample species. At low concentrations we can essentially stop the reaction from continuing at a certain point in the reaction by limiting the possibility of multiple sample species coming in contact with one another.

While these attributes of matrix isolation cause it to be quite a useful method for mechanistic study of gas phase reactions, there are a few drawbacks to matrix isolation which hinder its ability to be considered an identical reproduction of gas phase chemistry. The three main types of interactions that the matrix might impose can be categorized as physical effects, cage effects and chemical effects. As the physical and chemical effects mainly affect the quality of the resulting IR spectrum they are discussed in further detail when applicable in the following section on FT-IR matrix isolation.

Cage effects however directly impact the actual reaction pathway of a given molecule. An excited gas phase molecule proceeding along a dissociative

pathway will normally dissociate quickly with the fragments being displaced in space. However the same reaction occurring in a condensing matrix will experience a quite different outcome. The rigidity of the forming matrix will cause two major effects. Before dissociation can occur, the matrix material can deactivate the excited molecule through collisional deactivation. This will lower the energy of the molecule and remove the energy needed to dissociate. Furthermore it may be possible that the molecule will still dissociate. However, because the rigid matrix has formed around the parent molecule the fragments may be trapped in close proximity, causing them to recombine.⁵

1.1 FTIR Matrix Isolation

For absorption of infrared radiation in a molecule to occur, vibrational normal modes must become excited. These modes correspond to vibrations in the molecule either through stretching of the bonds or through non-stretching modes such as: bending, torsion, wagging, and deformations (these will be known as bending modes here). The number of vibrational modes can be easily calculated through knowing the number of atoms, N , contained in the molecule through the relation $3N-6$ for a non-linear polyatomic. Another key aspect of infrared spectroscopy is the fact that only the vibrational modes which result in a change in dipole moment of the molecule will be observed in the resulting spectrum. Vibrational spectroscopy has been studied in a large amount of detail and the information comprised by Wilson, Decius and Cross is a comprehensive guide.⁹

The position of the absorption bands for stretching features of small molecules are easily modeled, as an oscillator between two nuclei within the molecule while ignoring the motions of the other nuclei. The position can be solved in the expression from the solution to the harmonic oscillator problem¹⁰:

$$\bar{\nu}_{stretch} = \frac{1}{2\pi c} \sqrt{\frac{k}{\mu}} \quad \text{Eq. 1.1}$$

Where c is the speed of light in a vacuum, k is the force constant of the bond in motion and μ is the reduced mass for the two nuclei making the bond. Bending or deformation modes are quite complex in nature and may involve the movement of many nuclei within the molecule. This means that there is no one simple calculation for predicting the absorption position within the infrared. As the stretching motions can be considered to be involving only specific nuclei within the molecule they are ideal for identifying a given molecule as they can tell you what functional groups make up the molecule. This method is known as the group frequency approach and can be utilized because key functional groups will always have similar spectral ranges in which they appear. Key functional groups used in this study involve degrees of saturation, metal-carbon groups and metal hydride groups. The degree of saturation of a small hydrocarbon can be easily seen through C-H stretching mode region in the IR, as this stretching region will shift. This is best seen in the comparison of ethane, ethene and ethyne.

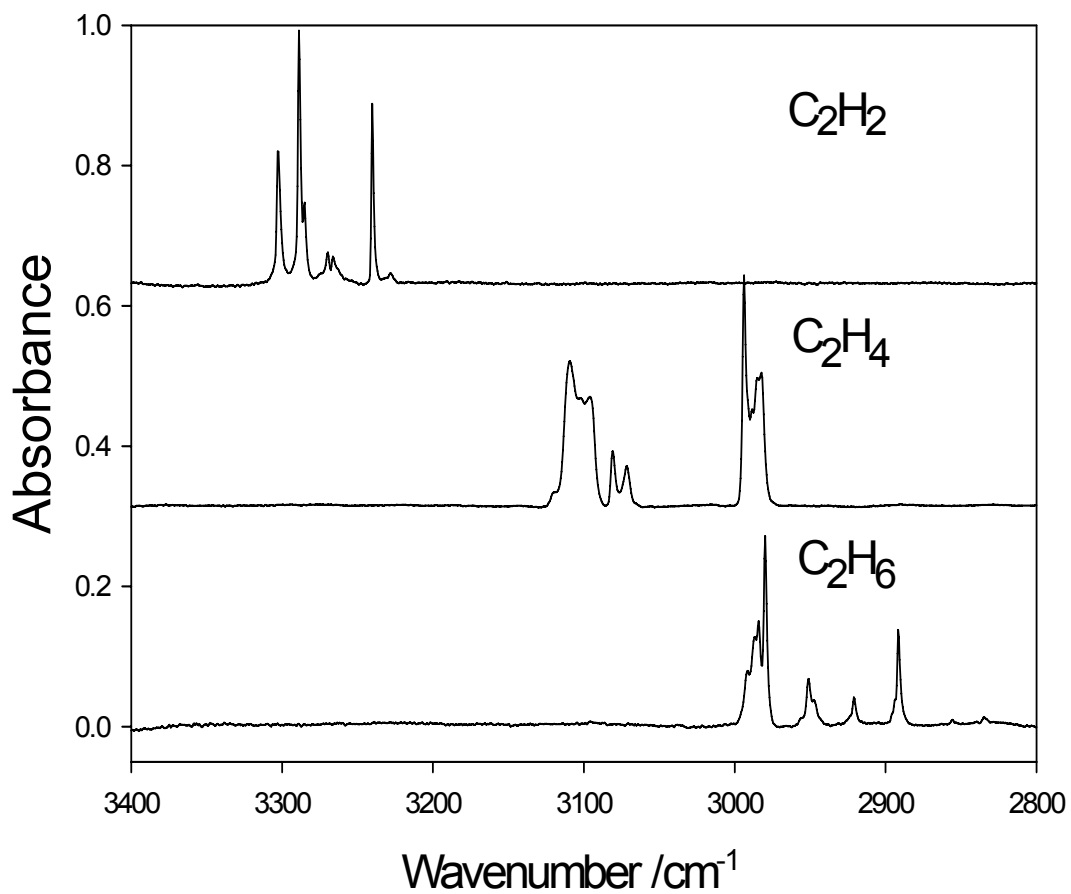


Figure 2: Infrared spectra of the C-H stretching region of matrix isolated ethyne (C₂H₂), ethene (C₂H₄), and ethane (C₂H₆). Note that spectra are offset for clarity.

While this approach is very useful for assignment of modes of the molecules trapped in the matrix it is not enough to fully identify the products. Further investigation using isotopically substituted analogs as well as computational models are necessary. As vibrational modes are dependent on the force constant and the mass of the species involved, using an isotopic substitution becomes a viable way to analyze and characterize the type of feature that gives rise to a particular mode. Nakamoto¹¹ shows that it is possible to predict the spectral shifting of a given stretching band through isotopic substitution (using equation 1.1). Taking the ratio of the observed vibrational wavenumber for hydrogen over deuterium you find that all factors cancel except for that of μ .

$$\frac{\bar{\nu}_H}{\bar{\nu}_D} = \frac{\frac{1}{2\pi c} \sqrt{\frac{k}{\mu_{H-X}}}}{\frac{1}{2\pi c} \sqrt{\frac{k}{\mu_{D-X}}}} \quad \text{Eq. 1.2}$$

Where μ_{H-X} and μ_{D-X} are the corresponding reduced masses of H and any other atom X and a D with X, this can then be reduced to:

$$\frac{\bar{\nu}_H}{\bar{\nu}_D} = \frac{\sqrt{\mu_{D-X}}}{\sqrt{\mu_{H-X}}} = \frac{\sqrt{2}}{\sqrt{1}} \quad \text{Eq. 1.3}$$

Because the mass of deuterium is twice that of hydrogen leading to that the ratio of a stretching mode of a hydrogen-X over deuterium-X as approximately 1.4. For many motions this ratio will not be exactly 1.4 as it is an approximation and for bending motions it may be as low as 1.10.

Using these tools infrared spectroscopy can be a very useful method for spectroscopic identification of chemical compounds. Troubles arise, however, in that in the gas phase thermal energies cause the molecules to occupy many different rotational states, causing broadening over a large range. This broadening can cause difficulty in identifying the product as key information may become hidden within the broad range. Matrix isolation, however, eliminates this problem by hindering the ability of molecule to rotate. This is generally a beneficial situation as it lowers the bandwidth of the peaks due to the removal of the P and R branches. However a situation where a percentage of the molecules will be held by the matrix in an orientation that is different to that of the others most likely will occur. This physical effect of the matrix will cause a small shifted peak that will be seen in the spectrum.¹² Both of these aspects, the small bandwidth and the shifting, can be seen well in Figure 3, below comparing gas phase SO₂ and SO₂ in a N₂ matrix, reproduced from Dunkin. Also, when higher concentrations of sample species are used, it is possible that you will form molecular aggregations. This may be what is sought when trying to promote a reaction between sample species; however, it may cause unwanted interactions which may complicate the spectrum, forming complexes that are not involved in the reaction under study. It is also true that matrix isolation will not fully stop small molecules from rotating within the site; however, due to the limited energy available only the first few rotational states will be populated and this should not limit the ability to identify any products.¹²

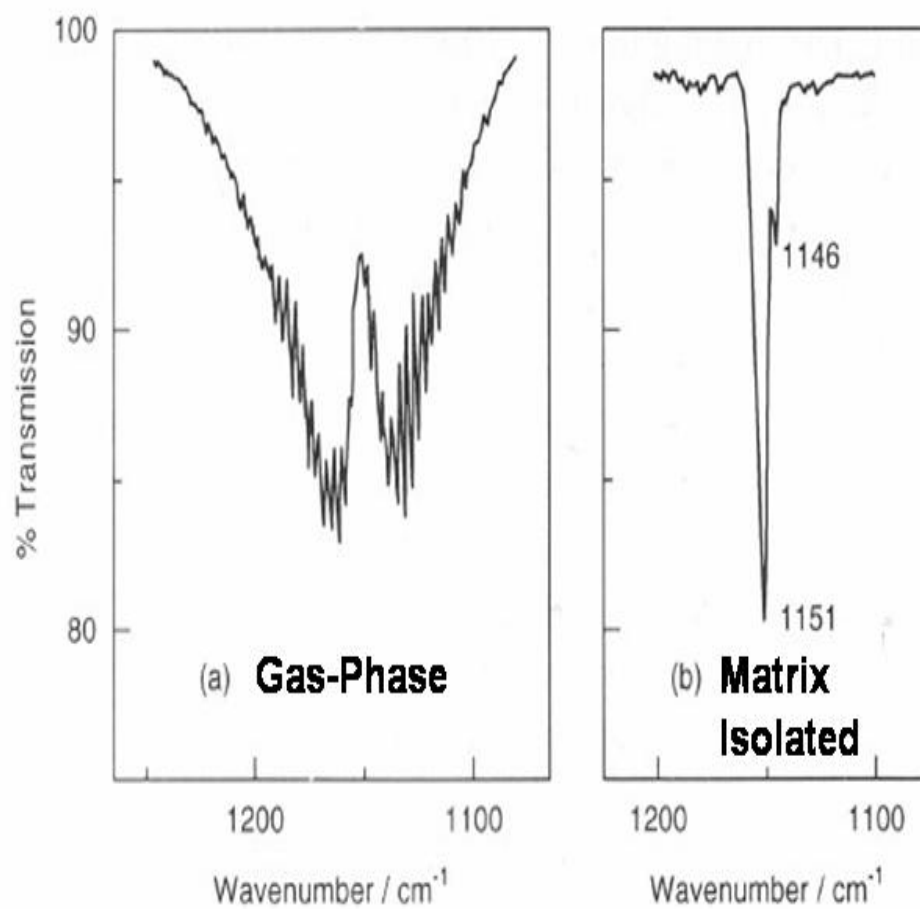


Figure 3: Comparison of the SO₂ IR modes both in the gas phase (a) and the matrix isolated section (b) it is possible to see the splitting of matrix isolated band due to a sample of the gas being confined in a different environment to that of the rest of the gas. Reproduced from Dunkin.¹²

Chemical effects caused by the matrix itself also cause changes in the IR spectrum with respect to that of a pure gas phase reaction. Usually, an inert gas, such as a group 8 gas, is used to limit these effects. Nevertheless, there remain measurable effects seen through electronic absorption. Neon has shown to have the lowest amount of interaction with most chemical; however, due to its low freezing point and relative expense it is usually replaced by argon.¹² The properties which make argon a useful matrix material have been discussed above.

There are further effects of vibrational spectroscopy which inherently cause additional features or the movement of a feature to a new position. There are several situations which may cause these effects; discussion here will revolve around overtone bands, coupling, and Fermi resonances.

In the harmonic oscillator approximation only transitions from $v = n$ to $v = n + 1$ are allowed and infrared active. However as molecules do not act perfectly harmonic, modes which are caused by transitions from $v = n$ to $v = n + k$, where k is an integer greater than one, are possible. These modes are known as overtones and correspond to integer multiples of the fundamental frequency ie. $2\nu_i, 3\nu_i, \dots$, these modes however are usually quite weak as the deviation from the harmonic oscillator is usually quite small. Along with overtones, combination bands are also possible. These are where a new vibration may become activated through combining with another.¹³ For example you may have $\nu_i \pm \nu_k$ or $2\nu_i \pm \nu_k$; these modes may help in identifying what motions belong to each mode as

they identify which features of the molecules are connected through particular bonds.

Fermi resonances causes the movement of bands from their suspected position to new locations. This effect is caused when a fundamental vibration and another mode either an overtone or a combination frequency are at or close to the same transition energy. This causes these two states to act degenerately and they will appear to repel each other, causing one band to be shifted to higher energies while the other is shifted to lower energy. Fermi resonances can only occur within the same species and can not affect other species in the area. Additionally, the intensities of both the fundamental and overtone bands are affected when Fermi resonances occur. The intensity of the fundamental band will shrink while the overtone which is normally quite small in intensity will grow. The result of these effects will cause additional features in the spectrum as there will be the original band along with the Fermi resonance bands. By identifying the Fermi resonance bands one can eliminate some of the possible unknown frequencies that may occur in the spectrum.¹³

Coupling effects cause splitting of bands, generating multiple bands where only one would be expected. It is caused by coupling of nuclei of the same mass within the molecule. When there are equivalent bonds in close proximity for example in methane CH₄, the stretching mode should appear in one location as all four bonds are equivalent. However coupling leads to the C-H bonds responding to one another. This motion removes the degeneracy of the vibration,

resulting in new absorptions at both higher and lower energy than the absorption for the degenerate motion of the molecule. One way to test if an absorption is caused by coupling is to repeat the experiment using a isotopically substituted molecule. By changing the mass of one of the nuclei that are coupled the coupled vibrations will be removed and a new absorption will become apparent. This new feature will be located at the average distance of the two coupled vibrations.^{11,13}

While these aspects of infrared spectroscopy do cause many complexities within the resulting spectrum, understanding how they occur and what they reveal makes it possible to use them to help identify the structure of a given molecule.

References For Chapter 1

- ¹ *The Organometallic Chemistry of the Transition Metals*, 4th Ed, Crabtree, R. (ed.); John Wiley & Sons, Inc.: Hoboken, NJ, **2005**.
- ² Parnis, J.M.; Escobar-Cabrera, E.; Thompson, M.G.K.; Jacula, J.P.; Lafleur, R.D.; Guevara-Garcia, A.; Martinez, A.; Rayner, D.M. *J. Phys. Chem. A.*, **2005**, 109, 32, 7046.
- ³ Thompson, M.G.K.; Parnis, J.M.; *Inorg. Chem.*, **2008**, 47 (10), 4045-4053.
- ⁴ Whittle, E.; Dows, D.A.; Pimentel, G.C.; *J. Chem. Phys.*, **1954**, 22, 1943.
- ⁵ Moskovits, M.; Andrews, L.; *Chemistry and Physics of Matrix Isolated Species*, Elsevier, New York, **1989**.
- ⁶ Fridgen, T.D.; Parnis, J.M.; *J. Phys. Chem. A.*, **1997**, 101, 28, 5117.
- ⁷ Kaye, G.W.C.; Laby, T.H.; Bullard, E., *Tables of Physical & Chemical Constants*, 13th Edition, Longman Group Limited: London. **1966**.
- ⁸ Moskovits, M.; Ozin, G.A., *Cryochemistry*, Wiley, New York, **1976**.
- ⁹ Wilson, E.B. Jr.; Decius, J.C. and Cross, P.C.; *Molecular Vibrations: The Theory of Infrared and Raman Vibrational Spectra*, Dover, New York, **1980**.
- ¹⁰ Atkins, P.W.; *Molecular Quantum Mechanics: An Introduction to Quantum Chemistry*, Clarendon Press: Oxford. **1970**.
- ¹¹ Nakamoto, *Infrared and Raman Spectra of Inorganic and Coordination Compounds Part A: Theory and Applications in Inorganic Chemistry*, 5th Edition, John Wiley and Sons. **1997**

¹² Dunkin, I.R. *Matrix isolation techniques: a practical approach*; Oxford University Press; New York, **1998**.

¹³ Herzberg, G. *Infrared and Raman Spectra of Polyatomic Molecules*, Van Nostrand Reinhold Company: New York, **1988**.

Chapter 2

Literature Review

2.0 Brief introduction of transition metal reactivity

A large amount of research into the chemistry of the transition metal elements has already been explored. It has been seen that as one moves from group to group along the periodic table the chemistry varies dramatically. In order to generalize trends seen within the transition metal series, the elements have been separated based on their apparent chemistry. The transition metals on the left of the table (Sc-Mn) are known as the early metals and those to the right are known as late transition metals (Co-Cu). This classification is somewhat generalized due to that fact that those in the middle of the table will sometimes act as early or late depending on the situation. The difference in chemistry is best explained by the change in effective nuclear charge. As one moves from left to right there is an increase in nuclear charge Z this is offset by an equal amount of electronic charge. However, the new electrons fill the vacant d-orbitals, which do not penetrate deeply into the nucleus. This causes an incomplete shielding of the nuclear charge leading to an increase in the effective nuclear charge (Z_{eff}) as one moves toward the late transition metals. This increase is the main cause of the variation of chemistry between groups. Another factor leading to additional diversity with respect to reactivity is caused by the high degeneracy of the orbitals in the metals. This leads to an increase in the number of low lying electronic states that are easily populated, each new state representing a unique

species. In general, the chemical differences between elements in the transition metal series are best characterized by orbital occupancy and the electronic configuration.¹ For further discussion of general aspects of transition metal inorganic chemistry the works of Cotton and Wilkinson² and Crabtree³ are excellent references.

2.1 Transition metal chemistry with hydrocarbons

The reactivity of transition metals with hydrocarbons is a widely studied area, the majority of which has been conducted in the solution phase. There has been, however, a considerable amount of work done involving gas phase reactivity of transition metals with hydrocarbons. A benefit of gas phase work is that, due to the lack of solvent, more comprehensive computational analysis is possible. The work discussed in this review will focus mainly on the reactivity towards alkenes. Propene (C_3H_6) in particular is discussed in detail.

A large general introduction to gas phase chemistry of transition metal ions and neutral atoms with hydrocarbons is summarized by Weissarr.⁴ Metal ion work is considerably more developed than the corresponding work with neutrals. Ions are more easily controlled and detected than neutrals and they are also considerably more reactive in most cases. For example, Weissarr has conducted a comparison of the reactivity of transition metal neutral atoms with singly and double charged ions, the results of which show considerably more reactivity towards the ions than the neutral atoms. Along with this, it is shown that

the specific reactions occurring are different between the ions and the neutrals. Weisshaar's account finds that the neutral gas phase transition metal interactions with hydrocarbons are typically repulsive at long range. Metal ions, however, tend to polarize approaching hydrocarbons causing an attractive force between the induced dipole in the alkene and the charge of the metal ion. The repulsive interactions of neutral atoms are more representative of solution phase chemistry where solvation effects lead to the net charge on any metal centre rarely ever reaching a true charge of 1+ or 2+.

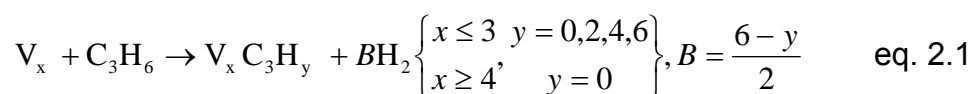
2.2 Gas phase reactions of transition metals with hydrocarbons

2.2.0 Cluster Chemistry

Parnis and coworkers have studied ethene reactions with niobium atoms and clusters containing up to 25 atoms.⁵ Clusters formed through a laser ablation technique were reacted with ethene through a fast flow reactor and analyzed with a time of flight mass spectrometer. They were also able to monitor the rate of cluster depletion with respect to reagent amount allowing for measurement of absolute kinetic rate constants for the reactions. Their work indicates that both niobium clusters as well as individual metal atoms were able to take up several ethene molecules sequentially. Individual metal atoms were shown to react with up to six ethene molecules, leading to products consistent with dehydrogenation of up to 5 H₂ units. Also performed by the group were computational DFT

calculations, which were shown to be in agreement with experimental findings of dehydrogenation of ethene.

Previously, reactions of small vanadium clusters with propene and propene halides have been studied by Song and coworkers.⁶ Metal clusters were formed through a laser vaporization process, exposed to propene in a fast flow reactor and detected by time of flight mass spectrometry. Findings with propene were similar to that of ethene. Dehydrogenation was shown to be the key process occurring in the reaction. Mass data indicated that several dehydrogenated products were formed corresponding to the loss of 2, 4, and 6 hydrogen atoms from any one particular propene molecule. The results also indicate that when clusters were of 4 vanadium atoms in size or larger that full hydrogenation was seen and only V_xC_3 , where $x \geq 4$, was the only product. Under the experimental conditions used in this experiment only one propene molecule was ever seen to interact with any given cluster. The general reaction equation seen throughout this work is summarized in equation 2.1 below.



2.2.1 Transition metal atom reactions with acetylene and other alkynes

Hinrichs and coworkers have investigated the competition between C-C and C-H bond activation in propyne and in 2-butyne when reacting with early second row transition metals.⁷ Metal atoms were formed using laser vaporization and the reactions were investigated using a crossed molecular

beam apparatus. Laser induced fluorescence was used to characterize the resulting electronic-state populations. H₂ elimination was found to occur with propyne in all of the ground electronic transition metal reactions studied, that is with Y, Zr, Nb, and Mo. Elimination reactions lead to a metal coordinated C₃H₂ group and H₂, and it was also seen that in the reaction with Y, CH₃ elimination was seen leading to a MC₂H complex. CH₃ elimination was only seen when collision energies of 69 kJ/mol or higher were used, below this only H₂ elimination was seen. The researchers theorize that the increase in reactivity of Y over the other elements towards CH₃ elimination was due the increase in bond strength of Y-CCH compared to that of the other metals. They do, however, note that they do not have any experimental or theoretical bond strengths for these systems. Reactions with 2-butyne showed that both CH₄ and H₂ elimination were present with Y, Zr, and Nb. Reactions with Mo showed only H₂ elimination.

Similarly Glendening has studied dehydrogenation reactions involving Y with acetylene.⁸ Potential energy surfaces are predicted and investigated for H atom and H₂ elimination. Only one pathway was found to be thermodynamically favorable for H₂ elimination. The process involves three steps whereby a YC₂H₂ adduct is formed, followed by C-H insertion and finally 1,3-elimination of H₂. The process is seen to be exothermic by 29.7 kJ/mol with the highest energy barrier found being in the 1,3-elimination step at 4.2 kJ/mol. H atom elimination is found to be an endothermic reaction by 62.8 kJ/mol. The computational work seems to generally agree with previous experimental investigations. Stauffer et al. conducted experimental investigations into the reactions of Y with C₂H₂ using

crossed molecular beams coupled with photoionization detection.⁹ H atom and H₂ elimination are seen under experimental conditions that agree well with computational data. There are some discrepancies between the two works with regard to the overall reaction mechanism and the overall energies of the reactions. 62.8 and -29.7 kJ/mol are reported in the computational data while the experimental research reports energies of 89.9 and -77.4 kcal/mol for H atom elimination and 1,3 elimination of H₂, respectively.

Competition between C-C and C-H insertion in cyclopropane reactions with Y, Zr, Nb, and Mo have been explored by Hinrichs et al.¹⁰ Using a rotatable source molecular beam apparatus and time of flight mass spectrometry the group was able to identify the branching ratios. Findings showed that C-H insertion was favored for Nb and Zr, whereas Y shows a slight tendency towards C-C bond insertion. Excited state Mo was also studied and it was found that C-C insertion was highly favored. This was then compared with the relative ab initio calculations for the barrier heights and good agreement between the two methods was seen. For the cases that favored C-C bond insertion it was also found that increase in collision energy increased the branching ratio towards C-C insertion.

2.2.2 Reactions of metal atoms with ethene and propene

A computational and experimental investigation of ground state Y with propene and ethene has been explored by Porembski and Weisshaar.¹¹ Their experiments investigated the reaction of the metal with propene in a fast-flow

reactor system, which was then analyzed by a time of flight mass spectrometer. The results for propene show the main products being YC_3H_4 and H_2 with a small amount of YC_3H_2 and $2H_2$ also being formed. Repeated experiments using C_3D_6 revealed that there was no kinetic isotope effect for the reaction towards propene. Contrasting to this are the results with ethene where although the major product is a dehydrogenation process similar to propene, there was a normal kinetic isotope effect detected for ethene. Computational results presented were only conducted with ethene. The findings show that once the metal complex forms it then inserts into the C-H bond where H_2 elimination occurs through 1,3 elimination. The other proposed mechanism, stepwise C-H bond insertion followed by H_2 elimination, was discounted. This is because the calculations showed that this process has energy barriers that would be above the available thermal energy under the experimental conditions used. Finally the authors also point out that reaction efficiency for $Y + C_3H_6$ was found to be higher to that of $Y + C_3H_4$, 16% vs. 1% respectively.

Previously Wen et al. conducted a study of the H_2 elimination products of the reaction of propene and ethene with Zr and ZrO.¹² The reactants are again reacted in a fast flow reactor, ionized by photoionization and detected through time of flight mass spectrometry. Reactions with low flow of propene showed evidence for production of ZrC_3H_4 as the major product in accordance with dehydrogenation. At a higher flow of propene, it was seen that ZrC_6H_8 is the major product indicating loss of 2 H_2 units from two propene molecules. Results for ethene show similar chemistry. Rate constants were developed for each

reaction; the bare metal reacting with C_3H_6 and the ligated metal ZrC_3H_4 reacting with C_3H_6 . Experimental observations show an increase in the rate of the reaction with ligands present. However, it is noted that this may be caused by increase in lifetime of the product as there are more degrees of freedom available to dissipate any internal energy, which may cause dissociation back to reactants in the nonligated reaction. The results from this paper suggest that 1,3-elimination of H_2 is a likely mechanism for the dehydrogenation of ethene; however, this is not discussed in the paper as this process had not been postulated at the time of publication.

Willis et al. also conducted a study involving the reactions of Nb and Zr with ethene.¹³ The study was conducted using a crossed molecular beam apparatus and measured with photoionization mass spectrometry. The findings show evidence for C-H bond insertion followed by dehydrogenation. The only difference found between the two metals was that Nb was found to be more reactive. This increase in reactivity is accounted for by the $5s^1$ outer shell of Nb compared to the $5s^2$ of Zr. The full outer s-orbital of Zr is much more repulsive towards the π bond of ethene at long range reducing reactivity.

Experiments determining kinetics data for the reactions of most transition metals with small hydrocarbons has been explored. Effective rate constants have been determined for these reactions using fast flow reactors with laser induced fluorescence and time flight mass spectrometry to monitor products. Ritter et al. have investigated the kinetics of first row neutral transition metal reactions with

small hydrocarbons.¹⁴ There is a difference seen between the reactivity of propene when compared to ethene. It is seen that ethene reacts with none of the first row neutral transition metal atoms except for Ni, whereas propene reacts with each of the early transition metals Sc, Ti and V, along with also reacting with Ni. The reactivity towards Ni is explained through the fact that Ni contains a low lying excited state which is accessible under thermal ambient conditions. It is proposed that the reactivity found is likely due to reactions involving this excited state ($3d^9 4s^1$) rather than the ground state ($3d^8 4s^2$). Late metals (Cr-Cu) except for Ni showed no reactivity towards propene and similarly very limited reactivity towards all other alkenes studied. Co showed very slight reactivity towards 1-butene and 1,3-butadiene. The lack of reactivity of late metals towards alkenes is attributed to long range repulsion effects. A full 4s outer shell will repel the incoming alkene, reducing the ability of it to reach the small vacant d orbitals, which are needed for complexation. In addition to this, the metals Cr through Co have enough electrons to partially fill all of the d orbitals. This increases the repulsion between the alkene and the metal atom, reducing the likelihood of reactivity.

Products of the reactions involving propene are suggestive of H_2 elimination after complexation with the metal. However, it is noted that it may be possible that the elimination is actually occurring through the reaction of a metal ion. This may be possible if the ionizing laser ionizes unreacted free metal atoms, which then go on to further react with the alkene. While they are unable to rule out this possibility it seems that the results are still in accordance with the initial

products being metal alkene complexes. Further investigation of the kinetic data showed no evidence of a kinetic isotopic effect for the reaction of propene with Sc, Ti and V. Ni however, showed a negative kinetic isotope effect. A proposed reason for this negative isotope effect is that if the reaction is a bimolecular elimination proceeding through a long lived metal-alkene complex this would produce a negative isotope effect. This would occur if the rate for dissociation back to reactants is larger or comparable to the rate of elimination. Reasoning for the absence of a kinetic isotope effect for Sc, Ti and V is also supportive of bimolecular elimination. This absence indicates that the first step is the formation of a complex between the metal and alkene which is long lived followed by insertion and subsequent elimination.

Further study of early first row transition metal reactions with propene and ethene have revolved around comparison of the kinetics of ground and excited state metal atoms. Senba, Matsui and Honma have studied the depletion rates of ground and excited state Ti and V atoms by propene and other small hydrocarbons.¹⁵ Metal atoms were formed using a discharge source with a cathode made out of the metal of choice. Atoms were carried through the flow tube to the reaction area where they were reacted with propene and analysed using laser induced fluorescence. Only ground state and first excited state (Ti a^5F ($3d^34s^1$), and V a^6D ($3d^34s^2$)) were studied. Results for propene suggest that while both the ground states of Ti and V react with propene, the excited state metal atoms react much more readily. As a measure of reactivity the ratio between the hard sphere rate constant and the experimental rate constant for the

given reaction are shown. Ratios $k_{\text{hs}}/k_{\text{exp}}$ are reported as 67 and 49 for ground state of Ti and V, respectively, while the excited states yield ratios of 1.6 for Ti and 2 for V. This indicates that excited state Ti and V reactions seem to be on the order of one in every two collisions. When compared with the results from ethene, excited state metal atom reactions occur just as frequently. Titanium a^5F yields a ratio of 1, while V shows a $k_{\text{hs}}/k_{\text{exp}}$ of 4 towards reactivity with ethene. Ground state metals however show no reactivity with ethene. Activation energies for the reactions with the hydrocarbons were calculated from the rate constants assuming the process follow Arrhenius behavior. E_{max} for propene show values of 1.3 kJ/mol for Ti a^5F and 1.7 kJ/mol for V a^6D . The results from this study show good agreement between this and the results from Ritter¹⁴. Increase in reactivity of excited state metal atoms seen for both ethene and propene is explained through the decrease in repulsion between the metal and alkene. This is due to the promotion of one of the s orbital electrons into a d orbital allowing for a higher possibility of M(alkene) adduct formation. It is suggested that the increase in reactivity of propene compared to ethene is caused by an avoided crossing between two low-spin surfaces in the case of propene. This avoided crossing is proposed to occur between the energy surface between the reaction of the ground state metal atom and a low lying state that is low spin and a $4s^1$ configuration, Ti b^3F ($3d^34s^1$) and V a^4D ($3d^44s^1$). Because these two surfaces have the same spin multiplicity they may be strongly avoided, causing a lowering in the activation energy. It is proposed that this lowering is enough to allow the reaction to occur in propene while it remains too high in the case of ethene.

The reactivity of second row transition metal atoms with linear alkenes has been further explored by the Weissarr group.^{16,17} The reactivity of the second row metals towards all alkenes studied is found to be greater than that of the first row. Ethene was found to react with all second row metals except for Mo and Ag while it did not react with any early first row metals. Propene, which does show reactivity with early first row metals, shows an increase in the rate of reaction when reacted with metals from the second row. Like ethene, propene reacts with all second row metals except for Ag while it does show very limited reactivity towards Mo. Nb is found to be the most reactive of all second row metal towards all alkenes studied. Results indicate that the reactions occurring are similar to that of the chemistry of the first row metals with propene. The increase in reactivity is likely due to the fact that the s and d orbitals are more similar in size than in the case of the first row. Additionally most of the elements in the second row do not have a full 5s outer shell, increasing the likelihood for the ability to complex with an alkene. Computational work done in the Weissarr study focused solely on ethene.¹⁶ The work again supports H₂ elimination; however, the calculations do not include a direct 1,3 elimination pathway from insertion into the C-H bond. Instead, the calculations focused on the ability of further insertion and formation of a H₂M...C₂H₂ complex which then eliminates H₂. Thompson suggested that it is possibly more likely that a direct 1,3 elimination pathway is occurring as many other works have suggested that it is quite an active elimination pathway.¹⁸

Some third row transition metals have been investigated with propene by Carroll and Weisshaar, again using a fast flow kinetics experiment.¹⁹ Reactions of Hf, Ta, Ir, Pt, and Au were with propene and other alkenes. Results indicate that again propene is seen to have a higher rate of reaction towards these metals than ethene, with the exception of Ir. Reactivity is found with all metals studied for both ethene and propene except for Au in each case. The rate of reaction with the third row seems to be in between the rates for the first and second row with the exception of Ta which is slower than both V and Nb. Also Pt is found to be faster than any other metal in its group. No products were identified in the work and further research is needed to make claims about the reasoning for the differences in the rates of reaction. It is not useful to use simple electronic configuration arguments in this case as the situation is much more complex for the third row metals than in the second or first rows.

Through these previous works it can be seen that transition metal reactions with hydrocarbons has been quite well characterized in the gas phase. There are some areas however in which these studies are lacking, specifically in the area of determining mechanistic process which govern these reactions. The majority of the gas phase work reveals only the depletion rates of metal atoms in the reactions, and the only information about possible products is through mass data. While this information is very useful, further analysis is needed in order to get a full structural and mechanistic description of the processes. To gain information about these valuable aspects, matrix isolation has been used. These

studies are aimed at isolating and characterizing the products formed throughout the reactions of transition metal atoms with simple hydrocarbons.

2.3 Metal atoms in inert gas matrices

The interesting and dynamic chemistry of transition metals seen in both the solution and gas phase has led to further research by matrix isolation. In order to study the nature and chemistry of transition metal atoms through matrix isolation, one must first be able to generate the metal atoms in the gas phase. A few different techniques have been developed for the purpose of generating metal atoms that can be deposited into a matrix. Generally, once the equipment has been developed for this purpose the steps to generate the atoms are simple, since maintaining the system is not an issue.^{20,21} The two main methods for generation of metal atoms in a matrix that are used today are laser ablation of the metal and vaporization of the metal through resistively heating a metal filament. Hollow cathode discharge sources are also sometimes used however their use is quite limited.

The laser ablation technique for generation of metal species to be deposited in a matrix is the newest method used. It has been seen that with the vast amount of power generated at such a focused point it is possible to vaporize most metals easily. The method was first developed by Knight et al. in 1986²² for the generation of B₂ molecules and B atoms, which were analyzed through ESR. Shortly after this laser ablation was also used by the Andrews group²³ for the

generation of Boron, studying the chemistry of B atoms with molecular oxygen. The technique was then adapted for the use with transition metals by both Andrews²⁴ and Zhou²⁵. Vaporization occurs by impinging a metal target with a focused laser. This high energy vaporizes the metal on the surface of the shot, resulting in a plume of metal atoms. The high energy also creates metal ions as well as many electrons. These additional species lead to the generation of some excited state metal atoms and negatively charged species along with the ground state species. This leads to complications when trying to determine mechanistic properties of the data, as situation is quite complex. It is, however, quite useful for the purpose of creating and analyzing unique organometallic species.

For mechanistic studies, thermal generation of metal atoms through resistively heating a metal filament under vacuum is usually used. Evaporation of metal atoms through resistively heating has been well documented.²⁶ Metal wires were originally used; however, due to the high heat generated, melting of the wires caused difficulties in the experiments. Metal filaments, while more durable than wires, need higher current in order to generate the needed temperatures for vaporization. As this method generates atoms through thermal vaporization the atoms generated are all neutral and in their electronic ground state. However, as the metal filament is heated it acts as a blackbody emitter and glows throughout the experiment. This bathes the matrix along with the metal atoms with light. Thompson has shown that the light produced may have sufficient energy to excite V metal atoms.¹⁸ Although it is not possible to discount the possibility of photoinduced chemistry in metal filament experiments, the lack

of highly excited atoms and ions allows for this method to be used in mechanistic studies quite well.

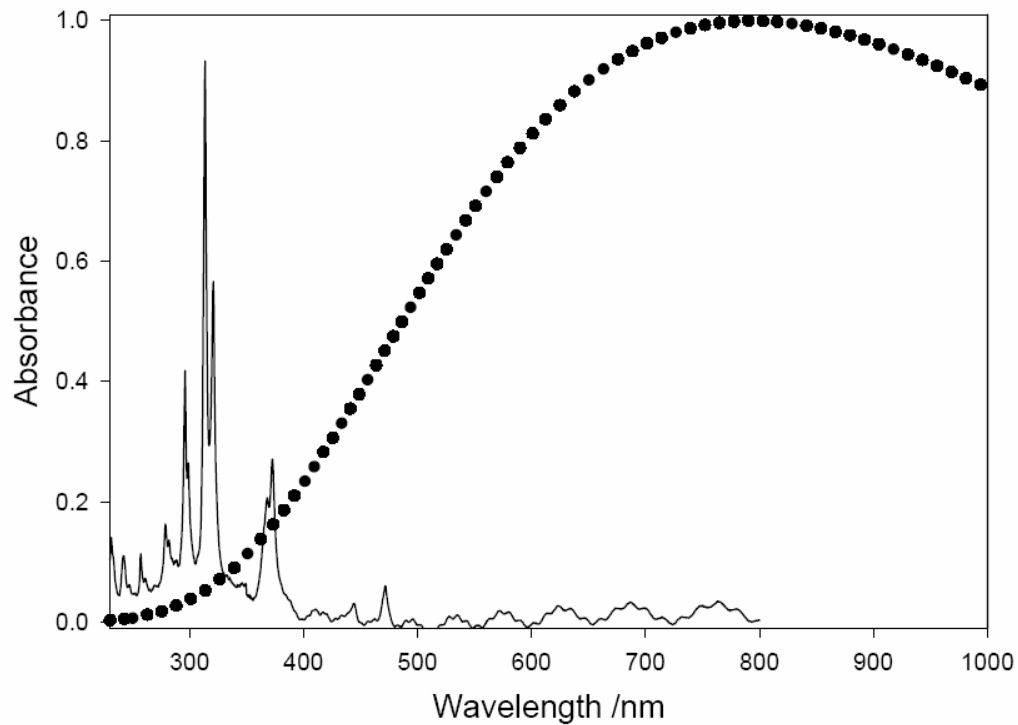


Figure 4: Comparison of the UV-visible absorptions of V atoms in an Ar matrix and the blackbody emission profile at 3680K which is the normal vaporization temperature for V. There is significant overlap of the feature at 375 nm along with 475nm. Reproduced from Thompson.¹⁸

In order to conduct experiments involving the chemistry of metal atoms with specific species such as alkenes, one must first identify any possible side reactions that may occur with the metals in the matrix environment. The two main chemical processes that occur as side reactions with metal atoms are reactions with water and formation of metal dimers. Water is known to contaminate most matrix isolation systems to at least some degree. This presents a problem as it has been seen that transition metal atoms generally react directly with water molecules under matrix isolation conditions. Kauffman has studied the reactions of water and all of the first row transition metal elements.^{27,28} Results indicate that all of the metals react spontaneously towards water. While all metals react with water it is also seen that they do not all react in the same way. Early transition metals are seen to insert into the OH bond of water while late metals form water complexes of the form $M-OH_2$.

For the early metals (Sc-V) Kauffman shows that there is no evidence for a $M-OH_2$ adduct in any of the three cases. It is stated that this is probably due to the short lived nature of the complex with these metals and that insertion occurs quickly. For all cases upon irradiation of the matrix with 300 to 400 nm light, the HMOH product decreases, MO is observed and H_2 or 2H elimination is then inferred. In the case of Sc, ScOH was also observed after irradiation as evidence for H atom abstraction. Additionally Kauffman also reports the reaction of metal atoms with two water molecules forming $H_2M(OH)_2$ upon condensation. This reaction is seen with all metals and does not increase upon irradiation. The formation of ScOH was confirmed by Zhang et al. who reproduced the

experiment using laser ablation techniques along with computational data.²⁹ The group also shows that further irradiation causes rearrangement of the ScOH molecule to HScO. The same group has also investigated the group IV³⁰ and V³¹ metal reactions with water using the same technique. Ti was found to react similarly to that found in the previous work by Kauffman with the addition of the observation of rearrangement to an H₂TiO complex before H₂ elimination. The second and third row elements in this group showed formation of H₂MO; however, no H₂ elimination was seen upon irradiation. The group V metals all have unique reactions towards water throughout their group. Vanadium is found to insert directly into the water molecule as reported by Kauffman. Irradiation of the matrix showed rearrangement to form H₂VO along with the formation of VO. Niobium reacts similarly; however, prior to irradiation a MOH₂ complex is formed before insertion. The results with tantalum showed no evidence for a formation of a MOH₂ adduct or HMOH however H₂MO was observed upon annealing of the matrix and no H₂ elimination was observed upon subsequent irradiation.

It is obvious from these works that the reactions of metal atoms with water molecules in the matrix environment are a possible source of observable and potentially reactive species within any matrix isolation experiment. The other side reaction of metals is the possible formation of metal dimers. This is an area which applies to the matrix environment and is not seen in gas phase chemistry.²⁶ Studies of the apparent chemistry of dimers are rather limited. Ozin et al. show that photolysis of the Co₂ dimer leads to two excited state atoms which can go on to further chemistry.³² The formation of dimer species has seen to be difficult and

this may explain the lack of study of the dimer chemistry. Characterization of the dimers has been explored through matrix isolation UV-Vis experiments similar that that of metal atoms.²⁰

2.4 Alkenes in inert gas matrices

The study of alkenes in inert matrices has been dominated by the significant study of ethene. As the simplest alkene it represents an archetypal molecule for the study of fundamental interactions with alkenes. The study of propene in matrix isolation is by comparison quite limited.

Barnes was the first to report a matrix isolation spectrum of propene in a Ar matrix.³³ This work is also the first to report ethene along with the butene isomers in a Ar matrix. The work compares its results with that of known gas phase spectra of the time. The results report many of the known fundamental bands and compares well with gas phase IR data. Along with propene, the allyl radical has also been investigated through polarized infrared absorption spectroscopy reported by Nandi et al.³⁴ Listed within the work are the calculated fundamental frequencies and the experimental vibrational frequencies for the allyl radical along with the perdeuterio and CH₂CDCH₂ isotopomers.

The matrix isolation study of propene with water has also been studied just as it has with transition metals. Engdahl and Nelander have studied the potential of water complexes with several olefins.³⁵ The O-H bond of water allows for hydrogen bonding with the π bond of alkenes. Propene shows similar

complexation to that seen with ethene in an earlier work by Engdahl.³⁶ The work lists the fundamental vibrations of the water propene complexes along with heavy water and HOD complexes. It is also shown that HOD does prefer to form a D bond with the alkene, which agrees with previous investigations with water and formaldehyde.

2.5 Reactions of metal atoms with simple hydrocarbons at low temperatures

The chemistry of metal atoms with hydrocarbons in inert matrices has again been dominated by the study of ethene with metal atoms. Thompson has given a thorough review of the known chemistry with ethene up to 2007.¹⁸ In general, the chemistry of transition metal atoms with ethene can be split into two areas. Those metals which only form a metal ethene complex with the π cloud of ethene along with other metals which insert into the C-H bond of ethene.

The most relevant of these studies to the current work was conducted by Cho and Andrews,³⁷ as it involves the group V metals. Generation of the metal atoms was conducted through laser ablation. Codeposition of the metals with ethene in Ar was recorded at 8K. Results show that the type of product formed in the reaction is dependent on the specific metal used. V shows no reactivity upon initial condensation; however, after irradiation considerable reactivity is seen. Formation of the initial insertion product ($\text{H-M-C}_2\text{H}_3$), the dihydrido complex ($\text{H}_2\text{M}(\text{C}_2\text{H}_2)$) and binary metal dihydride VH_2 are all seen to be present after irradiation. Upon condensation Nb and Ta both form the dihydrido product

however considerably more is formed after irradiation. Nb also forms a limited amount of the insertion complex (H-M-C₂H₃) and NbH₂, however, no evidence for these species is seen with Ta. The group also conducted experiments with CH₂CD₂ and found considerable scrambling occurring with all three possible isotopic forms of the dihydrido complex present. This finding is suggestive of β-hydrogen substitution within the insertion product.

Since 2007 a few additional studies have been done on ethene with metal atoms not covered by Thompson. In 2008, Cho and Andrews studied the chemistry of group VI metals with ethene using laser ablation techniques.³⁸ Again the observed products differ as one moves down the group. W and Mo show evidence for the formation of insertion (H-M-C₂H₃) and dihydrido complexes (H₂M(C₂H₂)) with ethene. Cr, however, is found to form the insertion complex as well as a metallacyclopropene complex. This product is proposed in the insertion mechanism to occur between the π complex and insertion. DFT results suggest that like the group V study the dihydrido complex becomes more stable as M varies down the group. H₂M(C₂H₂) is also again found to be the thermodynamically favored product. Unlike the group V studies, however, there was no evidence for a binary metal hydride, as no absorptions were found. This is postulated as evidence that H₂ elimination in these cases are slow and do not readily occur. The Cr dihydrido complex is assumed to not be easily formed, inhibiting H₂ elimination, and in the case of W and Mo it is proposed that the elimination step is slow.

Thompson and Parnis have since studied reactions of V with ethene and ethene water mixtures.³⁹ Metal atoms were generated using a resistively heated filament under high vacuum and condensed with C₂D₄ and water in Ar. Observed products differ based on the concentration of ethene present. When the ethene concentration was lowered, evidence for metal insertion into water is seen through H-VOH absorptions. Upon irradiation, subsequent hydrogenation of ethene to form CD₂H-CD₂H is seen and H-VOH absorptions decrease. At high concentrations of ethene and water alternative products were formed. Upon irradiation of the matrix the formation of C₂D₆ is evident and the formation of this must come from other ethene molecules as they are the only source of deuterium in the experiment. A mechanism involving sacrificial hydrogenation of one ethene molecule to another is proposed. A D-MCD₂ insertion product reacts with a second ethene molecule forming a π complex, which then inserts into the V-D bond. After formation of this CD₂CD-M-CD₂CD₃ complex, deuterium transfer and C₂D₆ elimination occurs, with a vanadium acetylene complex left. While the CD₂CD-M-CD₂CD₃ complex is not directly observed, the proposed mechanism is in agreement with previous research.

In comparison to the large amount of investigations into matrix isolated metal ethene reactions, similar studies towards propene are highly limited. Before discussing the metal propene reactions using matrix isolation, an investigation into metal allyl complexes should be discussed. In 1970, Bonnemann⁴⁰ conducted a low temperature NMR study on nickel allyl complexes. While this study is not directly a matrix isolation study the findings by

Bonnemann are used frequently to explain findings in matrix isolation studies. Results from the work show that there is a temperature dependent reaction between the π -allylhydridonickel complex and a propene-Ni complex. At temperatures below 223K, the allyl complex is favored and when the temperature is raised to 232K the hydrogen attached to the nickel transfers to the allyl group leaving a propene complex. The study further claims that when π -allyldeuterionickel is used, only the C1 or C3 atoms in the propene complex become deuterated. This is stated as a direct indication for a 1,3-H shift mechanism of isomerization.

Skell has researched metal reactions with propene by condensation of metal atoms emitted from a metal filament with propene along with other hydrocarbons. The first study involves the condensation of aluminum with a 100 fold increase of propene compared to Al, forming a propene matrix.⁴¹ Infrared results show an absence of any features that would be characteristic of Al-H bonds in the range of 1900-1700 cm^{-1} ; however, features at 700-600 cm^{-1} are indicative of Al-CR bonds. The condensate was heated and the excess propene pumped away and the product was then deuterolyzed with D_2O . The products from this reaction are indicative of the aluminum forming sigma type C-M bonds, as there is a high amount of D incorporation into propene. These results indicate the ability of propene to form direct C-M bonds with Al. Skell has also researched similar reactions with the transition metals Pt^{42} , Ni^{43} , and Cr^{44} .

Pt atoms were produced from their evaporation from a tungsten filament under vacuum, and they were then condensed with propene. Organometallic products were evident as the major product. The product was again deuterolyzed; however, unlike with Al, very little D incorporation was found. This gave evidence for a different type of complex being formed. No further analysis of the results are given as to what the specific structure could be other than the mention that it may be a π complex. When a similar study was conducted with Ni, results were similar to that of Pt as no incorporation of D was found after treatment of D₂O. Also studied in this work was the reaction of selectively deuterated propene and Ni. 2-Deuteriopropene and 3-deuteriopropene were condensed with Ni vapour in separate experiments. Interestingly, 3-deuteriopropene gave a mixture of 3-deuteriopropene and 1-deuteriopropene, along with non-deuterated propene. 2-Deuteriopropene, however, showed no evidence of scrambling and remained unchanged. The ability of the Ni complex to transfer the deuterium atoms in this way is suggestive of the 1,3-H shift seen by Bonnemann⁴⁰. The fact that non-deuterated propene is observed is possible evidence that the process allows for inter- as well as intra-molecular exchange occurring. The 1,3-H shift is also proposed to occur in similar experiments in the same work conducted with 1-butene, in which evidence for both *cis*- and *trans*-2-butene were found.

Cr was found to show chemistry which is in between that what is found with Al and Ni. Where Al was found to incorporate D into propene after deuterolysis of the Al-propene complex and Ni lead to a complex unable to

incorporate D however it did show evidence for 1,3-H shifts. Cr is found to incorporate some amount of D into propene after deuterolysis albeit to a lower extent than Al. The researchers also suggest that 1,3-H shift with Cr through the allyl hydride mechanism is possible as like Ni the reaction with 1-butene and Cr leads to *cis* and *trans*-2-butene. It appears that the chemistry that occurs with Cr is somewhat between the extremes of Al and Ni.

Hisatsune reexamined the reaction of propene and Ni atoms as well as with Mg atoms.⁴⁵ Hisatsune condensed Ni atoms with propene in a similar manner to that was performed by Skell and then observed formed products using infrared spectroscopy at -190°C. This method allows for detection of any possible complexes directly as in the previous work no structure could be observed. Using 3,3,3 d-propene observation of hydrogen transfer was evident in the observed IR. Analysis of the IR shows that a 1,3-H shift is occurring as proposed by Skell; however, Hisatsune proposed that it is not occurring through a allyl intermediate as previously thought. Hisatsune finds no evidence for an allyl complex as no π -allyl nickel hydride was observed. Furthermore Hisatsune points out that the observed complex has absorptions more similar to that of the π -propene than the π -allyl species found by Dent when propene was absorbed onto a zinc oxide surface⁴⁶. Hisatsune suggests that a π -propene intermediate is the most likely formed intermediate and that it is also able to perform a 1,3-H shift.

It can be seen that the mechanism and the products formed in the reaction of propene and metals needs further analysis. A few studies of the reactions of

propene with transition metal atoms in inert gas matrices have been done as an attempt to further study these processes. Kasai has studied propene complexes of the group 11 metals (Cu, Ag, and Au) using matrix isolation ESR⁴⁷. Parker et al. studied the reactions of iron with propene as well as ethene using IR alongside Mössbauer spectroscopy.

Kasai investigated the potential of the coinage metals to form complexes with propene, and no insertion products were ever found. Metal atoms were generated by resistively heating a tantalum cell containing the specific metal up to the evaporation temperature of the metal. The vapour was condensed with propene in either a Ar or Ne matrix material. Carrying on the general trend of transition metals in the gas phase, the chemistry varies between the metals as one moves down the group. Cu and Au are both observed to form monoligand structures with propene similar to that which was seen in an earlier study with ethene, that is a π complex with the double bond of propene interacting with the metal. At higher concentrations of propene both of these metals appear to form a M-dipropene complex in the bisligand formation. Ag, however, seems to deviate away from the chemistry seen with ethene. Ag atoms were found to only form a complex with the bis(ethene) system and no observation of the monoligand complex was found. When Ag atoms were reacted with propene, however, there were only signs of weak associations with propene and neither a monoligand complex or a bis(propene) complex appeared to form. The weak bonding between propene and Ag is proposed to occur due to the stability of the d orbitals compared to the other metals. As the energy levels of the valence d orbitals in Ag

are low, at -11.32 eV, compared to -9.11 and -10.36 eV for Cu and Au, respectively, the d electrons have a decreased interaction between a π^* orbital of propene. Kasai also reports the EHT (Extended Huckel theory) orbital energy calculations for the antibonding orbitals in ethene and propene. The π^* orbital of ethene was found to have an energy of -8.24 eV while propene is reported to have the π^* orbital energy of -8.06 eV. Kasai claims that the increase in energy of this orbital in propene may be why the bis(ethene) complex can form while the bis(propene) complex does not.

Parker, using Mössbauer spectroscopy, has studied the reactions of Fe with propene and ethene in a Ar matrix. Infrared spectroscopy was also completed for ethene. Iron atoms were generated through resistively heating a iron filament. The atoms were condensed with the alkene on a Be disk at 4K for Mössbauer interpretation and on a NaCl window at 16-20K for infrared analysis. The results show similar chemistry to that of Fe with either ethene or propene, as expected. Similar to the work done by Kasai, the alkenes formed a monoligand complex with the metal atoms, and no observation for a bis(alkene) complex was found, however. It is also observed that while in the reaction with ethene some unreacted Fe remained, all Fe was consumed in the reaction with propene. This is indicative of the reported increase in reactivity of propene in the gas phase, compared to ethene.

It is evident by the limited amount of previous studies on the reactions of propene and transition metals in inert gas matrices that much more research in

this area is needed. Specifically, the early transition metals show a very limited amount of research with propene. The lack of study in this area is surprising when compared to the amount dedicated to ethene, as gas phase studies show a large increase in reactivity of early ground state metals with propene compared with ethene. The remaining chapters discuss the observed products of the codeposition of propene with vanadium. This work aims to further explore the gas phase work seen with propene using matrix isolation, as none of the previous work seem to explore the H₂ elimination results from the gas phase.

References for Chapter 2

- ¹ Armentrout, P.B.; *Science*, **1991**, 251, 175.
- ² Cotton, F.A.; Wilkinson, G.; *Advanced Inorganic Chemistry*, 5th Ed.; Wiley, New York, **1988**.
- ³ Crabtree, R. (ed); *The Organometallic Chemistry of the Transition Metals*, 4th Ed, John Wiley & Sons, Inc. Hoboken, NJ, **2005**.
- ⁴ Weisshaar, J.C.; *Acc. Chem. Res.*, **1993**, 26, 213.
- ⁵ Parnis J.M.; Escobar-Cabrera, E.; Thompson, M.G.K.; Jacula, J.P; Lafleur, R.D.; Guevara-Garcia, A.; Martinez, A.; Rayner, D.M.; *J. Phys. Chem.*, **2005**, 109, 7046.
- ⁶ Song, L.; Freitas, J.E.; El-Sayed, M. A.; *J. Phys. Chem.*, **1990**, 94, 1604.
- ⁷ Hinrichs, R.Z.; Schroden, J.J.; Davis, H.F.; *J. Phys. Chem. A*, **2008**, 112, 3010.
- ⁸ Glending, E.D.; *J. Phys. Chem. A.*, **2004**, 108, 10165.
- ⁹ Stauffer, H. U.; Hinrichs, R. Z.; Schroden, J. .; Davis, H. F.; *J. Chem. Phys.* **1999**, 111, 4101.
- ¹⁰ Hinrichs, R.Z.; Schroden, J.J.; Davis, H.F.; *J. Am. Chem. Soc.* **2003**, 125, 860.
- ¹¹ Porembski, M.; Weisshaar, J.C.; *J. Phys. Chem. A.*, **2001**, 105, 6655.
- ¹² Wen, Y.; Porembski, M.; Ferrett, T.A.; Weisshaar, J.C.; *J. Phys. Chem. A*, **1998**, 102, 8362
- ¹³ Willis, P.A.; Stauffer, H.U.; Hinrichs, R.Z.; Davis, H.F.; *J. Phys. Chem. A.*, **1999**, 103, 3706
- ¹⁴ Ritter, D.; Carroll, J.J.; Weisshaar, J.C.; *J. Phys. Chem.*, **1992**, 96, 10636.

-
- ¹⁵ Senba, K.; Matsui, R.; Honma, K.; *J. Phys. Chem.*, **1995**, 99, 13992.
- ¹⁶ Carroll, J.J.; Haug, K.L.; Weisshaar, J.C.; Blomberg, M.R.A.; Siegbahn, P.E.M.; Svensson, M.; *J. Phys. Chem.*, **1995**, 99, 13955.
- ¹⁷ Carroll, J.J.; Haug, K.L.; Weisshaar, J.C.; *J. Am. Chem. Soc.*, **1993**, 115, 6962.
- ¹⁸ M.G.K. Thompson, PhD. Thesis, Queen's University, Kingston Ontario, 2007.
- ¹⁹ Carroll, J.J.; Weisshaar, J.C.; *J. Phys. Chem.*, **1996**, 100, 12355.
- ²⁰ Moskovits, M.; Ozin, G.A.; *Cryochemistry*, Wiley, New York, **1976**.
- ²¹ Dunkin, I.R.; *Matrix Isolation Techniques*, Oxford University Press, New York, **1998**.
- ²² Knight, L.B. Jr; Gregory, B.W.; Cobranchi, S.T.; Feller, D.; Davidson, E.R.; *J. Am. Chem. Soc.*, **1987**, 109, 3521.
- ²³ Burkholder, T. R.; Andrews, L.; *J. Chem. Phys.*, **1991**, 95, 12.
- ²⁴ Chertihin, G.V.; Andrews, L.; *J. Am. Chem. Soc.*, **1994**, 116, 8322.
- ²⁵ Zhou, M.; Zhang, L.; Dong, J.; Qin, Q.; *J. Am. Chem. Soc.* **2000**, 122, 10680.
- ²⁶ Moskovits, M.; Andrews, L.; *Chemistry and Physics of Matrix Isolated Species*, Elsevier, New York, **1989**.
- ²⁷ Kauffman, J. W.; Hauge, R.H.; Margrave, J.L.; *J. Chem. Phys.*, **1985**, 89, 3541.
- ²⁸ Kauffman, J. W.; Hauge, R.H.; Margrave, J.L.; *J. Chem. Phys.*, **1985**, 89, 3557.
- ²⁹ Zhang, L.; Dong, J.; Zhou, M.; *J. Chem. Phys. A*, **2000**, 104, 8882.
- ³⁰ Zhou, M.; Zhang, L.; Dong, J.; Qin, Q.; *J. Am. Chem. Soc.* **2000**, 122, 10680.
- ³¹ Zhou, M.; Dong, J.; Zhang, L.; Qin, Q.; *J. Am. Chem. Soc.* **2001**, 122, 135.
- ³² Hanlan, A.J.L.; Ozin, G.A.; Power, W.J.; *Inorg. Chem.*, **1978**, 17, 3648.

-
- ³³ Barnes, A.J.; Howells, J.D.R.; *J. Chem. Soc. Faraday Trans II.*, **1973**, 69, 532.
- ³⁴ Nandi, S.; Arnold, P.; Carpenter, B.K.; Nimlos, M.R.; Dayton, D.C.; Ellison, G. B.; *J. Phys. Chem. A.*, **2001**, 105, 7514.
- ³⁵ Engdahl, A.; Nelander, B.; *J. Phys. Chem.*, **1986**, 90, 4982.
- ³⁶ Engdahl, A.; Nelander, B.; *Chem. Phys. Lett.*, **1985**, 113, 49.
- ³⁷ Cho, H.G.; Andrews, L.; *J. Phys. Chem. A.*, **2007**, 11, 24, 5201.
- ³⁸ Cho, H.G.; Andrews, L.; *J. Phys. Chem. A.*, **2008**, 12071.
- ³⁹ Thompson, M.G.K.; Parnis, J.M; *Inorg. Chem.*, **2008**, 47, 4045.
- ⁴⁰ Bonnemann, H.; *Angew. Chem. Int. Ed.*, **1970**, 9, 736.
- ⁴¹ Skell, P.S.; Havel, J.J.; *J. Am. Chem. Soc.*, **1972**, 94, 22.
- ⁴² Skell, P.S.; Havel, J.J.; *J. Am. Chem. Soc.*, **1971**, 93, 6687.
- ⁴³ Skell, P.S.; McGlinchey, M.J.; *Chem. Internat. Edit.*, **1975**, 14, 195.
- ⁴⁴ Skell, P.S.; McGlinchey, M.J.; *J. Am. Chem. Soc.*, **1973**, 95, 3337.
- ⁴⁵ Hisatsune, I.C.; *J. Cat.*, **1982**, 74, 18.
- ⁴⁶ Dent, A.L., Kokes, R.J., *J. Am. Chem. Soc.*, **1970**, 92, 6709.
- ⁴⁷ Kasai, P. H.; *J. Am. Chem. Soc.*, **1984**, 106, 3069.

Chapter 3

Experimental

3.0: Materials

Gas Phase Materials:

Argon (Ar) – Praxair, Ultra high purity (5.0) 99.995%

Propene (CH₃CHCH₂) – Aldrich, 99+%

Propene-d₆ (CD₃CD₂) – C/D/N Isotopes, 99.7% atom D

Propene-3,3,3-d₃ (CD₃CHCH₂) – C/D/N Isotopes, 99.9% atom D

Liquid Phase Materials:

Water (H₂O) – No supplier, Purified through freeze pump thaw process

Heavy Water (D₂O) – Aldrich, 99% atom D

Metal Materials:

Vanadium (V) – Alfa Aesar, 99.99%

3.1 Gas Handling Line

Sample preparation is conducted on a stainless steel, high-vacuum, gas handling pipeline (Figure 5) free-standing from the matrix isolation apparatus.

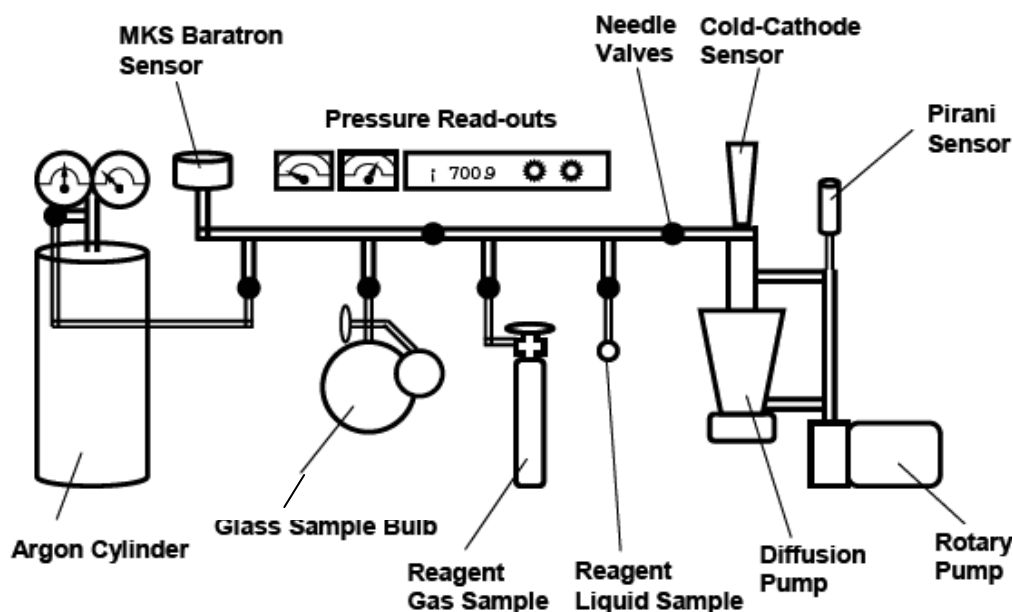


Figure 5: Gas handling pipeline used for preparation of gas samples

Vacuum in the line is achieved through a two stage pumping system. A rotary vane pump is used to first achieve pressures of 10^{-3} Torr. Once this is reached a diffusion pump is opened, reducing the pressure to approximately 5×10^{-8} Torr. The vacuum is measured for the two stages by two different gauges. A higher pressure range Pirani sensor is used to monitor pressures down to 10^{-3} Torr, which is the lower limit while under rotary vane pump conditions. The second is a cold cathode ion gauge which is sensitive between 10^{-4} and 10^{-9}

Torr. At pressures above this range, the gauge is unable to obtain accurate results and is turned off. In order to monitor the absolute pressure within the line, a MKS Baratron sensor is used during preparation of the sample. Needle valves are used in order to control the flow in and out of each terminal along the line. They can be manipulated to allow small amounts of gas through from the gas cylinders into the system. Gas sample cylinders, liquid samples and the argon cylinder are attached to the system using Ultratorr compression fittings. A further summary of pumping systems and gauges used in matrix isolation can be found in "Matrix isolation techniques: a practical approach", by Dunkin.¹

3.2 Preparation of Gas Sample

The sample bulb is first cleaned by evacuating with the vacuum pump. Once the bulb has been evacuated for at least a few hours and the pressure remains constant at an appropriate level (10^{-7} Torr), it can be used. In most cases, only two components were used in the sample, the host gas (argon) and the sample gas (propene and others). Once vacuum is achieved throughout the system it is sealed off from the pumps and the sample gas is delivered from the reagent cylinder to the gas bulb up to the appropriate pressure, as read by the MKS Baratron sensor. As the amount of argon needed in the bulb will be much larger than that of the sample, the partial pressure of argon will also be much larger, which is why it is introduced after the sample gas. The sample is diluted with

argon to the appropriate pressure. The calculation of the pressures needed is based on Dalton's law of partial pressure and treating the gases as ideal. As a demonstration for the preparation of a 800 Torr sample with a concentration of 1:100 propene to argon, 7.92 Torr of propene is added and then diluted to 800 Torr with Ar. By Dalton's law of partial pressure the partial pressure of argon is the total pressure minus the partial pressure of the propene. Thus, $P_{\text{Ar}} = P_{\text{t}} - P_{\text{propene}} = 800 \text{ Torr} - 7.92 \text{ Torr} \approx 792 \text{ Torr}$

From the ideal gas law $PV = nRT$ the mole ratio of the two species can be calculated as follows:

$$\frac{n(\text{propene})}{n(\text{Argon})} = \frac{P_{\text{propene}} V / RT}{P_{\text{Argon}} V / RT} = \frac{P_{\text{propene}}}{P_{\text{Argon}}} = \frac{7.92 \text{ Torr}}{792 \text{ Torr}} = \frac{1}{100}$$

*Note that because V, R and T are equal for each species, they cancel.

Samples that involve the use of liquid reagents at STP are obtained by using the vapour pressure of the liquid. The storage and treatment of liquid samples is different from that of the gas samples, which can be used directly from the lecture bottles. Liquid samples become exposed to the atmosphere which may allow for atmospheric gasses to become dissolved within the liquid. These gases must be removed from the sample prior to being introduced to the sample bulb. This is done through a freeze-pump-thaw degas process outlined below.

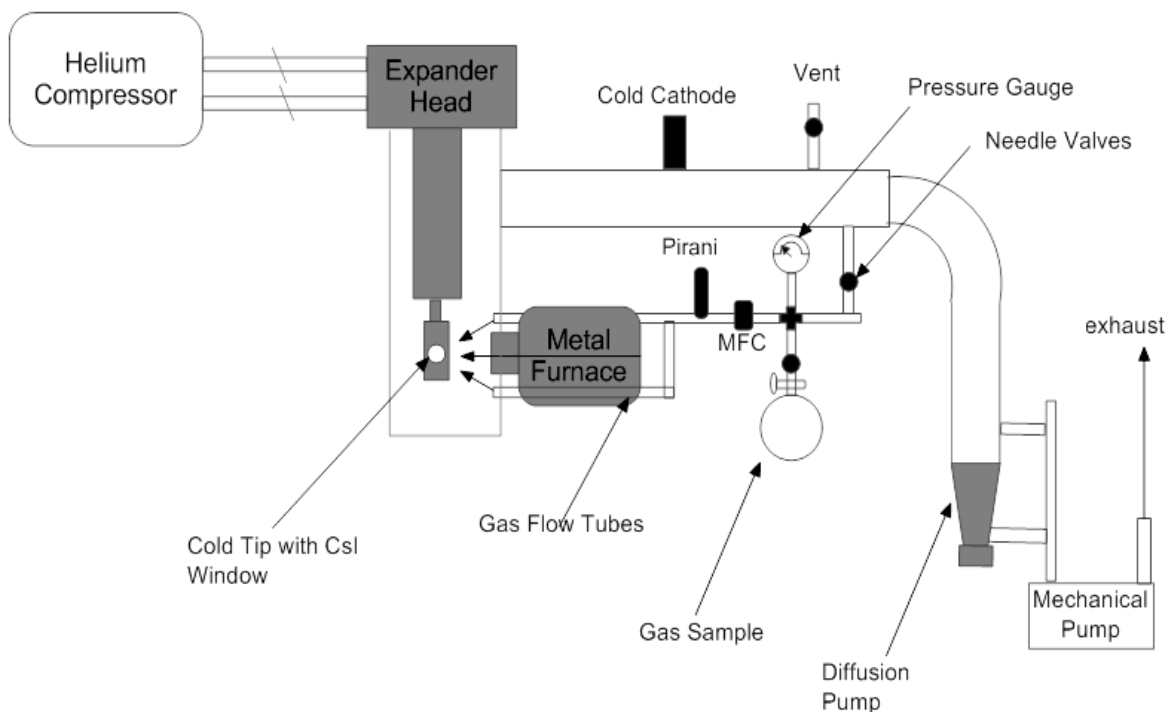
A small amount of the liquid is placed in a round bottom flask that can be connected to the gas handling line. It is isolated from the system using the

needle valve. The sample is then cooled using liquid nitrogen, and the sample is frozen. Any impurities that were not dissolved remain above the sample, and exposing the frozen sample to vacuum removes these impurities. The sample is isolated once more and is allowed to thaw. Impurities that were dissolved in the sample will move to the gas phase in order to return the system to equilibrium as described by Raoult's law. The process is repeated, as each successive time additional amounts of the impurities are removed and eventually the sample is purified. In most cases three repetitions are enough to purify the sample to a level that is needed.

Another key difference in liquid samples is that the vapour pressure of the liquid may become a limiting factor in the amount of gas that can be evolved from the sample. This is not a problem in this work where only water and its isotopes are used, as only a small amount is ever needed within the gas bulb (at most 10 Torr).

3.3 Metal Deposition Matrix Isolation Apparatus

A Schematic diagram of the metal deposition matrix isolation apparatus is seen below in Figure 6



*Note MFC= Mass Flow Controller

Figure 6: Schematic diagram of the metal deposition matrix isolation apparatus.

The cold tip and expander can be rotated such that it is possible to deposit, irradiate, and acquire a spectrum.

3.3.1 Vacuum System

The vacuum system of the matrix isolation apparatus is similar to that of the gas handling line. An Edwards E2M2 rotary vane pump evacuates the system down to 10^{-3} Torr, as measured by a Pirani gauge. This pressure is still too high to perform matrix isolation experiments. A diffusion pump is used to further pump the system down to 10^{-7} Torr, as measured by a cold cathode ion pressure sensor. This pressure is sufficiently low that the cooling system is able to maintain a constant temperature throughout the experimental process and limit the possible impurities.

3.3.2 Cooling System

Once the system is evacuated to an appropriate level, an APD Cryogenics Displex closed cycle helium refrigeration system is turned on. This system works throughout the “Expander head” in Figure 6 as a refrigeration cycle taking advantage of the Joule-Thompson effect. Helium gas is pumped into the evacuated section of the expander allowing it to expand and this cools the area down. It is then pumped out and it cycle repeats cooling it further. Continued cycles of pumping allow for cooling at the spectroscopic window (cold tip) down to 13K. At this temperature the pressure is lowered further from 10^{-7} to around 10^{-9} Torr.

3.3.3 Gas Handling within the Matrix Isolation Apparatus

Once the system has cooled, the gas sample is flowed towards the cold tip through the system. The pressure remaining in the sample bulb is measured using a helicoid pressure gauge. The flow of the gas is monitored and controlled through a MKS mass flow controller. Experiments were conducted through a range of flow rates varying from 0.5 sccm (standard cubic centimeters)/min through 2.5 sccm/min.

3.4 Reaction Chamber

A diagram of the reaction area and furnace assembly can be found in Figure 7. The chamber encloses the gas reaction zone, the metal furnace, the cold window upon which the gas condenses, the gas flow tubes, two radiation shields, along with two parallel CsI windows for spectroscopic analysis and a quartz crystal microbalance. For additional information on reaction chamber components, specifically, salt windows and the quartz crystal microbalance, “Cryochemistry”, by Moskovits and Ozin, is a good resource.²

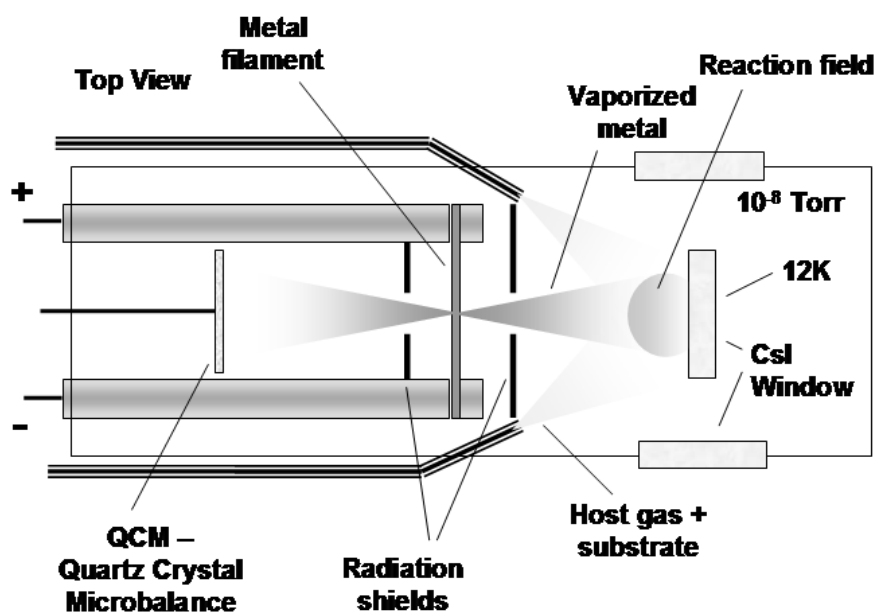


Figure 7: Schematic diagram of the interior of the reaction chamber used in the metal deposition matrix isolation apparatus. The electrodes are cooled with flowing water throughout the deposition.

3.4.1 Vaporization of metal atoms

The furnace assembly is given in Figure 7. The basic design involves passing an alternating current through the electrodes spanned by the metal filament. The electrodes are cooled through a constant flow of water. This cooling also cools the metal foil. Increasing the current through the metal eventually heats the centre of the filament up to the vaporization temperature of the metal. An aluminum radiation shield in front of the metal source acts to protect the matrix from the heat produced from the metal vaporization. Metal atoms produced from the vaporization disperse both forwards towards the cold window

and backwards towards a quartz crystal microbalance. Forward moving metal atoms that pass through a small hole in the radiation shield mix with the gas sample as it is passed through tubes towards the mixing zone. Here the metal atoms and the gas sample begin to react. The mixture eventually hits the cold window where they form the matrix condensed on a CsI window. Metal atoms sent in the other direction travel towards a second radiation shield used to mimic the other radiation shield. This ensures that the amount of metal atoms that reach the quartz crystal microbalance is the same as the amount that reaches the cold window and is also used to protect the crystal from the radiation of the metal filament.

3.4.2 Quartz Crystal Microbalance

In order measure the amount of metal atoms emitted from the filament a quartz crystal microbalance is used. A crystal with a nominal oscillation frequency of 5 MHz is used. As metal is deposited onto the surface of the crystal its mass increases. This causes the frequency of the oscillation to decrease. By measuring the amount by which the frequency has decreased it is possible to calculate the amount of metal deposited on the crystal. For the crystals used here the frequency decreases by about one cycle for every 20 ng deposited on the surface. This allows for the measurement of the amount of metal by the number of cycles per minute used (cpm). Because the distance to the quartz crystal microbalance and the cold tip are equal and that the sizes of the holes in

the radiation shields are known it is possible to calculate the amount of metal reaching the cold tip.

3.4.3 Metal filament preparation

The metal filaments were prepared by cutting a strip from pure metal foil (~5 cm long x ~0.5 cm wide x 0.1 cm thick). When preparing the metal strip gloves were used to prevent the introduction of oils onto the metal surface. The oils easily corrode early transition metals when heated. The metal was cleaned with methanol to remove any organics on the surface before being attached to the electrodes.

3.4.4 Spectroscopic Windows

In Figure 7 three windows can be seen; with two facing parallel and a third in the middle being perpendicular. The perpendicular window is the cold window, cooled by the expander. It can be rotated to be in line with the other windows. It is on the surface of this window that the matrix forms. The other two windows are used to admit the spectrometer beam. It is passed through the first window, then through the cold window (and matrix), and then through the final window and detected by the spectrometer. Cesium iodide is used for these windows as they are softer than other salt windows (not as brittle) and this limits the risk of fracture while tightening windows. They also have a broad spectral transmitting range needed for infrared analysis. The major disadvantage to CsI over other windows is that they are highly hygroscopic. This problem is avoided here in several ways.

First, the matrix window is kept under high vacuum for the majority of its life, lowering the risk of water vapour affecting the window. The other two windows are covered and have a dry nitrogen gas flow protecting them. Second, the degradation of the windows caused by water affects them by becoming cloudy. This effect only seems to scatter visible light leaving the IR range mostly unaffected.

3.5 Irradiation and annealing of matrices

Once the matrix has formed and a spectrum has been acquired it is possible to further manipulate the matrix to see if any changes occur. Irradiation of the matrix with ultraviolet and visible light can excite the metal atoms out of their ground state and if the metal atom has formed a complex or inserted into the sample species then this energy is dissipated through the molecule via molecular vibration. This added energy may be enough to help move a potential intermediate out of a small potential energy well and promote formation of further products. In this work a Kratos LH-150W Hg arc lamp was used with various filters to irradiate the matrices.

The temperature of the cold tip was monitored and controlled through a temperature controller. A temperature sensor located at near the cold window is used to indicate what the temperature of the system is. Typical temperatures for the system used ranged from 15 to 12K. A small heater is also attached to the tip

and is controlled through the temperature controller. This allows for heating of the matrix once it has formed, in order to anneal it. Annealing the matrix allows molecules that were trapped in a site which was not its lowest energy state to reach their preferred orientation. This helps to remove site effects. Another benefit of annealing is that after irradiation has occurred, a molecule that was trapped in a energy well may not be able to rearrange to its new potential minimum orientation, as annealing allows for this to occur. Typical annealing routines involve increasing the temperature to around 22K for 2-5 minutes.

3.6 Procedure for isotopic substitution work with water.

Water has the ability to exchange protons with other water molecules found in the same area. When doing isotopic substitution experiments with D_2O , care must first be taken to make sure that there is no H_2O found in the system that may exchange with the deuterium. In order to do this both the gas handling line and the matrix isolation apparatus must be treated with D_2O . Repeated exposures with D_2O vapour acts to eliminate as much H_2O as reasonably possible by exchanging with system H_2O .

References for Chapter 3

¹ Dunkin, I.R. *Matrix isolation techniques: a practical approach*; Oxford University Press; New York, **1998**.

² Moskovits, M.; Ozin, G.A., *Cryochemistry*, Wiley, New York, **1976**.

Chapter 4

Results

The generation and characterization of vanadium atoms in Ar matrices under similar experimental conditions using the same apparatus has been previously studied by Thompson.¹ The following chapter presents the experimental results generated from the investigation of the reactivity of vanadium atoms with propene. Also a study of the reactivity of a propene water system was conducted. The temperature of the matrix was maintained at around 14K for the duration of the deposition and while acquiring the spectra for all studies unless otherwise noted.

4.1 Vanadium reactivity towards propene in argon matrices.

Initial investigation of the reactivity of vanadium with propene was conducted upon deposition and following irradiation of the matrix. A mixture of 1:100 propene:Ar was co-condensed on a CsI window with 3 cycles per minute of vanadium for 60 minutes. Several new IR absorptions were seen upon deposition.

The resultant spectra with and without metal deposition are compared in Figure 8. In order to show the differences between the two more clearly, a difference spectrum is shown in Figure 9. Irradiations were performed using various filters on the matrix surface in order to investigate the impact of irradiation. A comparison of the infrared spectrum after several different irradiation exposures can be seen in Figure 10.

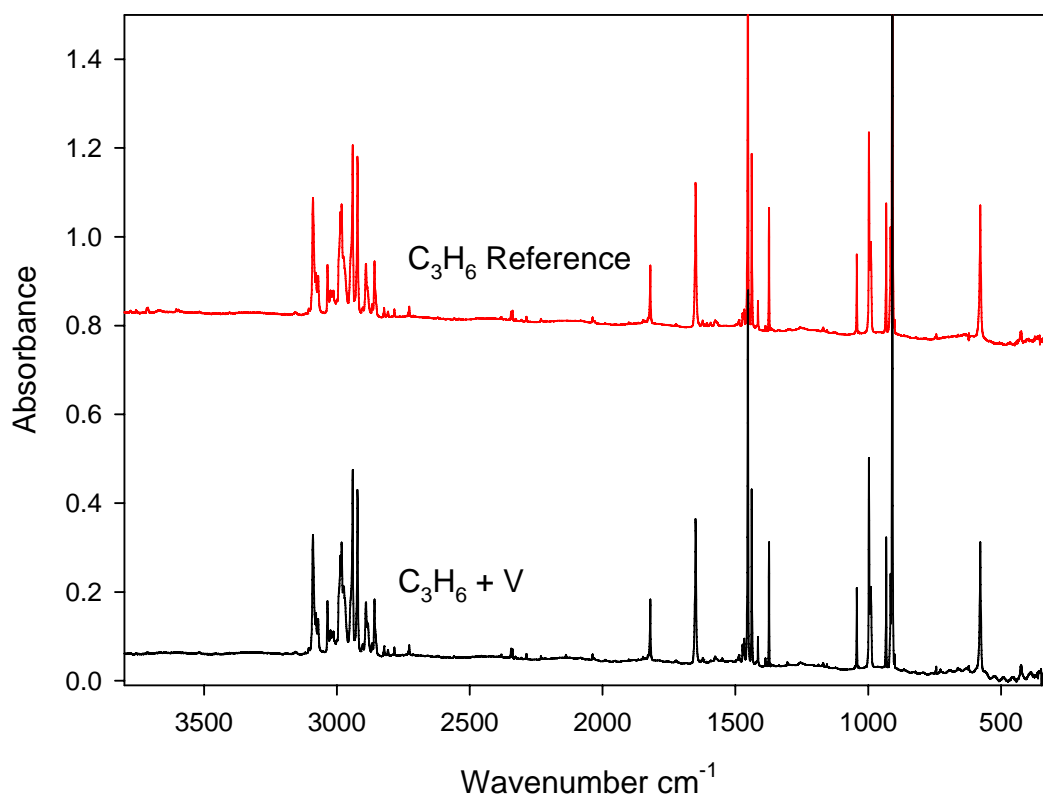


Figure 8: Full spectrum of C₃H₆ with and without metal present. 1:100 propene:Ar at 2.5 sccm/min, with vanadium was deposited at 3 cpm for the duration of the deposition. Note that the new features are very small and difficult to see in this image, so the difference spectrum in Figure 9 is provided for clarity.

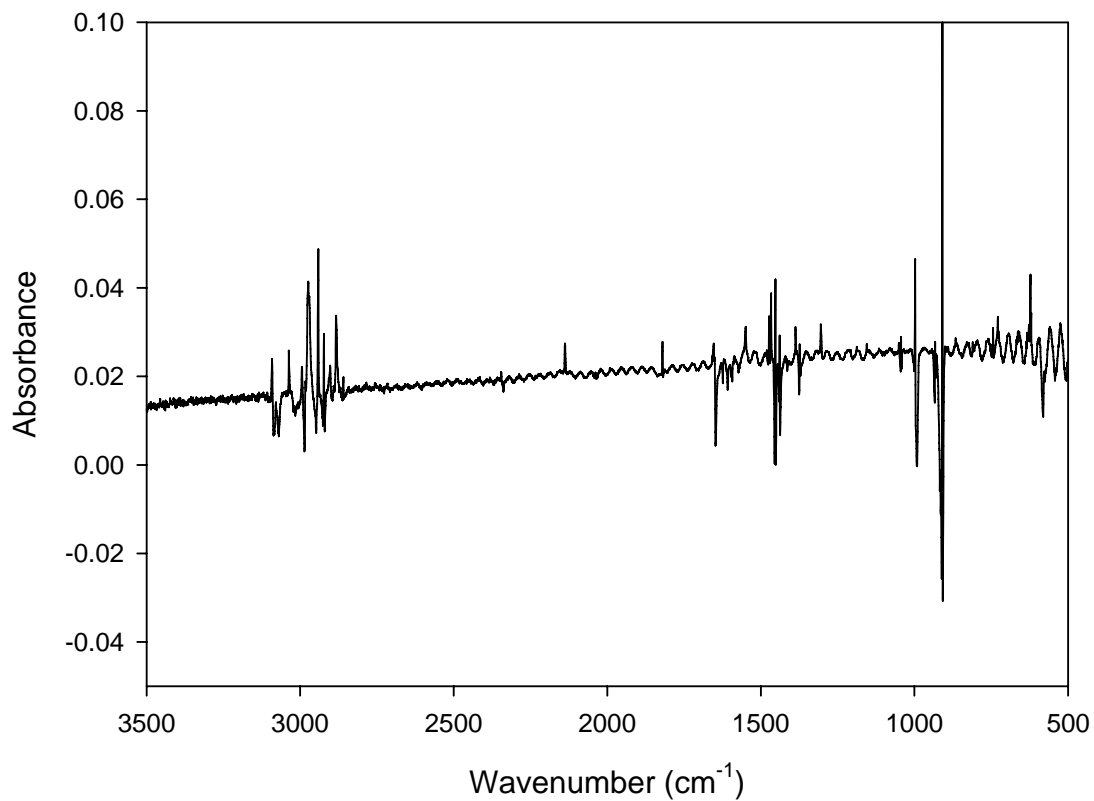


Figure 9: A difference spectrum of the reference spectrum subtracted from the deposition with 3 cpm of vanadium. The figure shows a number of product features as well as depletion of some features.

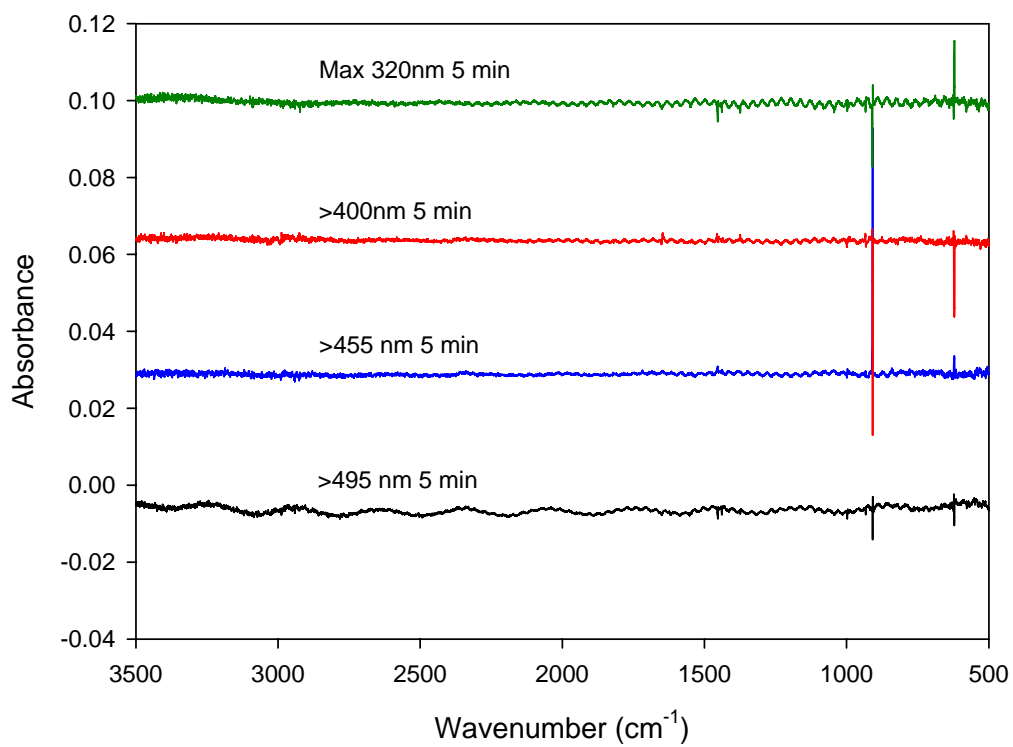


Figure 10: Irradiation at several different wavelengths of light shows very little change. Changes around 900 and 600 cm⁻¹, while appearing intense, are caused by very small insignificant changes of very intense features and the areas of both bands are quite small.

All propene and water features show a decrease in absorbance after deposition with metal atoms. As well, it is evident that many new features appear in the spectrum, suggesting one or more products.

Several of the new bands seen in the spectrum after deposition with V are similar to that of propane (2973.4, 2969.8, 2940.6, 2906, 2881, 1473, 1466, 1459, 1387, 1373, 1187, 1155, 1050, 865, and 744 cm^{-1}). In order to identify these features as propane a sample of propane diluted in Ar was deposited such that a comparison of matrix isolated propane and the products from the reaction is possible. Figure 11 shows that several of the features listed in Table 1 correspond to propane. Table 2 below shows the additional features that appear upon deposition that do not correspond to propane.

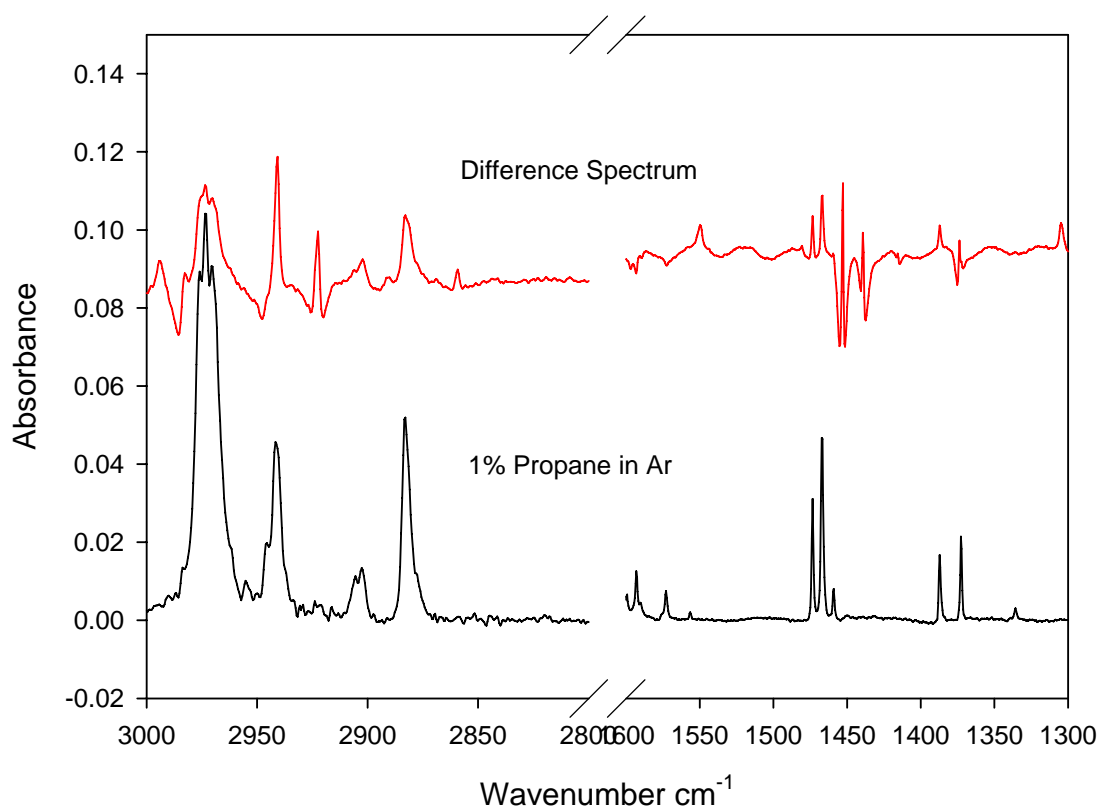


Figure 11: Comparison of matrix isolated and the difference spectrum obtained by subtraction of the reference from the deposit with vanadium. It can be seen that several of the new bands observed correspond to propane features.

Table 1: Wavenumber positions of new features in the resulting spectrum along with features that show a decrease in intensity following the reaction of V + 1:100 C₃H₆:Ar.

New features in Spectrum following deposition		Features that showed a decrease in intensity following deposition	
Wavenumber	Wavenumber	Wavenumber	Wavenumber
2973.4	1373	3714	1595.5
2969.8	1335	3711	1453
2940.6	1305	3088	1438
2906	1187.5	3072	1415
2901.8	1155	3033	1374
2881.6	1050	2988	1044
2137.9	909	2947	995
1548	865	2923	991
1480	810	2891	933.6
1473	744	2859	915
1466	728	1821.5	909
1459	633	1650	620
1387	622	1624	578
		1608	

Table 2: Wavenumber positions for the features following the reaction of V + 1:100 C₃H₆:Ar other than those corresponding to propane.

Wavenumber	Identity if known
2137.9	CO
1549	
1480	
1305	Methane
975	
810	
728	
622	

It is evident from the initial study of the reaction of propene and V that propane is the major product species. Along with propane, several other features are also present. In order to identify what causes the production of propane, optimization studies were carried out by varying the experimental parameters. This process also helps to identify which of the unknown bands are related to one another by analyzing how they change under different conditions.

The irradiation study revealed no changes in the matrix after irradiation with all wavelengths studied suggesting that there are no photochemically active species present after irradiation.

4.2 Optimization of Propene

Varying one of the experimental parameters while holding the others constant allows for the investigation of which conditions promote propane formation. The various conditions that were studied were propene concentration, metal flux, and the flow rate of the propene:Ar sample.

4.2.1 Variation of propene concentration

A sample of 1:50 propene in argon was codeposited with metal atoms at 3 cpm and analyzed in the usual manner. The sample was then diluted with argon to 1:100 propene to argon, and the process was repeated for 1:200 and 1:1000 propene to argon concentrations.

Figure 12 displays a plot of absorbance of several of the propane features that appear on deposition for the different concentrations. The general result from the study shows that propane formation is favored at higher concentration of propene. Conversely it was also found that a group of features also seen in the spectrum after deposition decrease as concentration of propene is increased. Figure 13 displays a plot similar to Figure 12 illustrating some of these non-propane features in order to find what conditions lead to their formation.

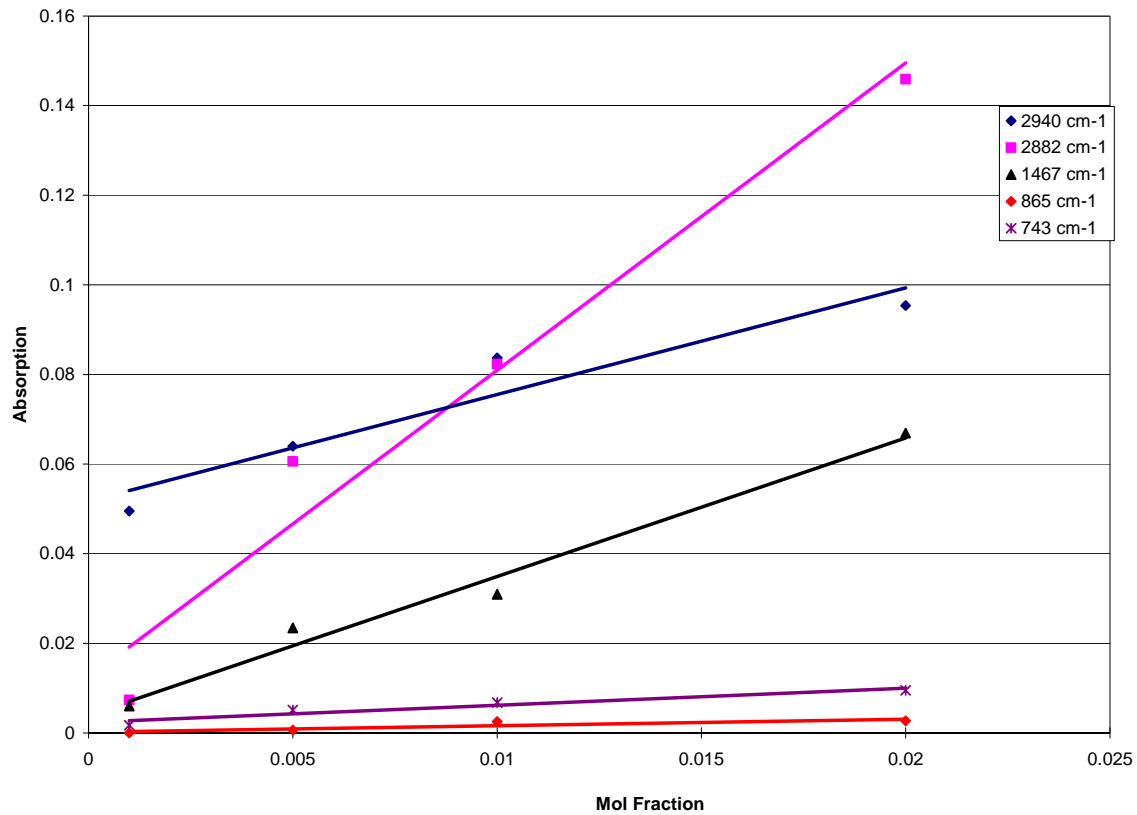


Figure 12: The normalized areas of several propane features from subtraction spectra are plotted against the mole fraction of propene to argon. It is evident that at higher propene concentration a higher proportion of propane is formed.

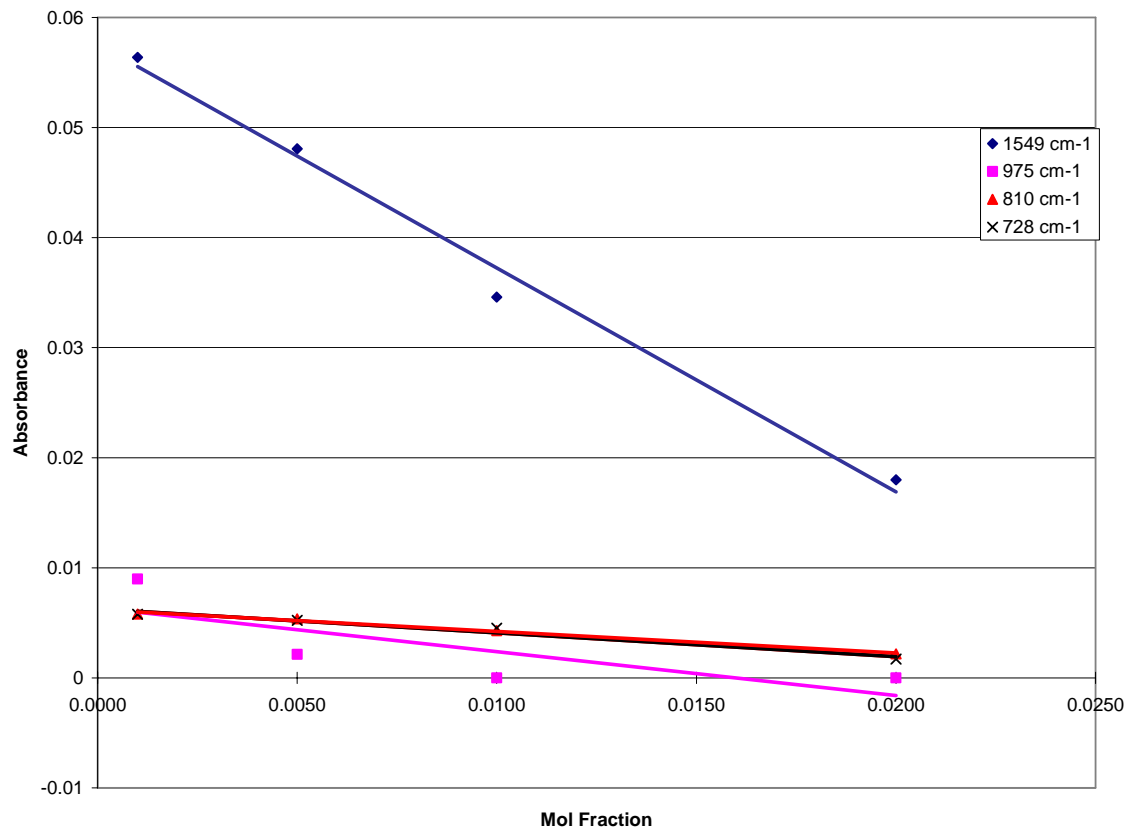


Figure 13: The areas of several non-propane features from subtraction spectra are plotted against the mole fraction of propene to argon. It is evident that these features track together and exhibit the opposite trend to that of propane.

4.2.2 Variation of metal flux

The variation of metal flux was studied under both high and low concentrations of propene. This allows for the best study of the effect of metal flow under conditions that favor propane formation along with the formation of the other product(s). Figure 14 compares the resulting difference spectrum after deposition with three different metal flows with that of a 1:100 propene:Ar sample. Metal flow rates studied were 3, 7, and 10 cpm of vanadium. In Figure 14 difference spectra are again compared from different metal flows. 1:1000 propene:Ar was used in order to try and promote the formation of the non-propane features.

It can be seen from the figures that both the propane and the non-propane features increase as the metal flow is increased. It is also seen that of the non-propane features many track well together. Features at 1549, 1480, 975, 810 and 728 cm^{-1} track together very well, while a feature at 1207 cm^{-1} also appears to track with the other features. However, its intensity is so low that it is hard to distinguish it from the noise and it is not shown in the figure.

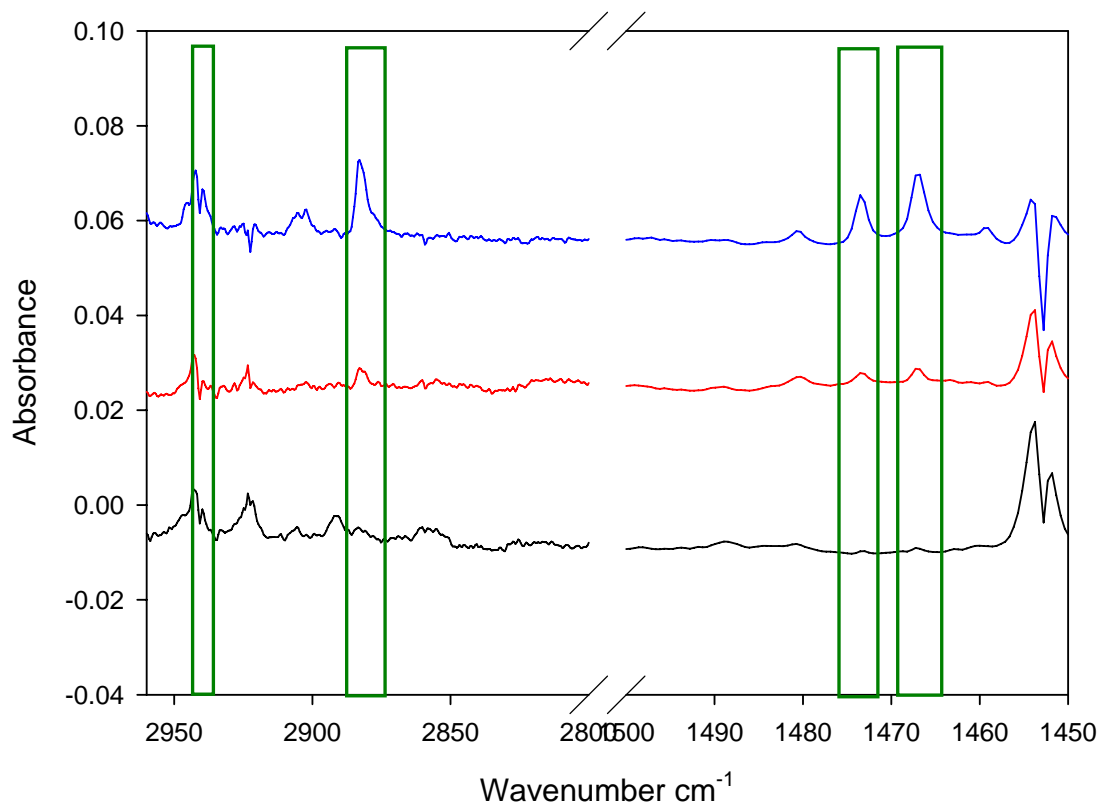


Figure 14: Selection of the infrared spectrum for 1:100 propene:Ar displaying the key regions for some of the propane features at three different metal flows; black 3 cycles per minutes, red 7 cpm and blue 10 cpm. Blocks indicate key features.

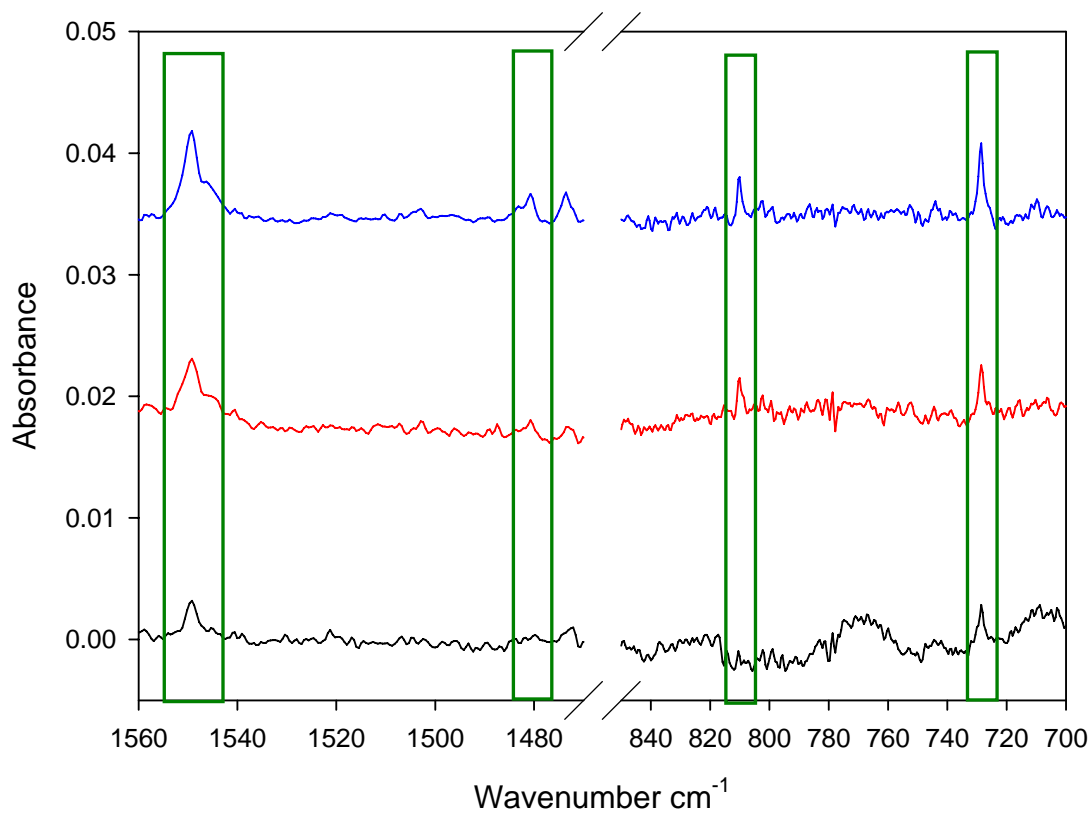


Figure 15: Selection of the infrared spectrum for 1:1000 propene:Ar displaying the key regions of the non-propane features at three different metal flows; black 3 cycles per minutes, red 6 cpm and blue 9 cpm. Blocks indicate key features.

4.2.3 Variation of gas flow

The variation of gas flow was studied under both high and low concentration of propene. This allows for the study of the effect of gas flow under conditions that favor propane formation along with the formation of the other product.

A sample bulb of 1:1000 propene to argon was condensed with V at several different flow rates (0.5, 2.5 and 5 sccm). Table 3 lists the integration areas of several propane and non-propane features. Using a higher concentration of propene to argon the process was repeated; however, flow rates of 0.5, 1 and 2.5 sccm were used in order to limit spectral congestion. Table 4 lists the integration areas of several propane and non-propane features at a concentration of 1:200 propene:Ar.

Table 3: The areas of several features that appear on deposition with V under several different flow rates. The last two columns give the ratios of the areas found at 0.5 sccm and 2.5 sccm vs. 5 sccm for 1:1000 propene:Ar.

Propane Features (cm^{-1})	0.5 sccm	2.5 sccm	5 sccm	5/0.5sccm	5/2.5sccm
2972	0.0128	0.0403	0.0944	7.3717	2.3414
2882	0.0015	0.0158	0.0291	18.7645	1.8313
1467	0.0009	0.0036	0.0076	8.2803	2.0475
743	0.0007	0.0016	0.0037	5.2719	2.3438
Non-propane Features					
1549	0.0060	0.0168	0.0343	5.7247	2.0387
975	0.0014	0.0041	0.0094	6.8989	2.2677
810	0.0014	0.0043	0.0077	5.6580	1.7955
728	0.0040	0.0058	0.0094	2.3563	1.6124

Table 4: The areas of several features that appear on deposition with V under several different flow rates. The last two columns give the ratios of the areas found at 0.5 sccm and 1.0 sccm vs. 2.5 sccm for 1:200 propene:Ar.

Propane Features (cm^{-1})	0.5 sccm	1 sccm	2.5 sccm	2.5/0.5sccm	2.5/1sccm
2972	0.0366	0.0761	0.1825	4.983	2.3995
2882	0.0084	0.01620	0.0491	5.809	3.0330
1467	0.0060	0.0086	0.0193	3.2310	2.2357
743	0.0030	0.0064	0.0096	3.1672	1.4956
Non-propane Features					
1549	0.0169	0.0250	0.0509	3.0077	2.0411
975	0.0065	0.0026	0.0032	0.4930	1.2316
810	0.0088	0.0111	0.0331	3.7559	2.9670
728	0.01808	0.0273	0.0565	3.1255	2.0722

When looking at the non-propane features it is evident that three of the four peaks studied, 1549, 810, and 728 cm^{-1} , track well together throughout the different conditions. The peak at 975 cm^{-1} is seen to track well in the low

concentration range however it does not at the larger concentration. It is possible that this is caused by the fact that at this concentration the peak is quite small that calculating the area becomes quite difficult. As the other non-propane features are found to be strongest at low concentrations of propene, and as under these conditions the feature tracks well, this feature will be treated as though the feature tracks with the other features listed above. It is also evident that the features at 1207 and 1480 cm^{-1} also track well with the first three features above, although they are not included in the table.

Through the optimization studies it is seen that propane formation occurs readily under higher concentration of propene while an additional product(s) appears at lower concentrations. Flow rate appears to have little effect on the production of either propane or the additional product(s).

As all of the different experimental condition experiments show that several of the non-propane features track well under all changes of conditions, it can be taken as evidence for the assertion that these features are caused by one product, which is known as the additional product from here forward. In order to gain further structural information of this additional product and mechanistic information of the formation of propane, an isotopic substitution study was carried out.

4.3 Reactions of V with isotopes of propene: V + C₃D₆ and C₃D₃H₃

4.3.1 Reaction of V with C₃D₆

Figure 16 shows portions of the IR spectrum obtained after deposition of V with 1:100 C₃D₆:Ar. The absorptions observed following deposition and their possible identities are given in Table 5. Several of the new features occur in similar positions to those found in the gas phase infrared spectrum of C₃D₈.²

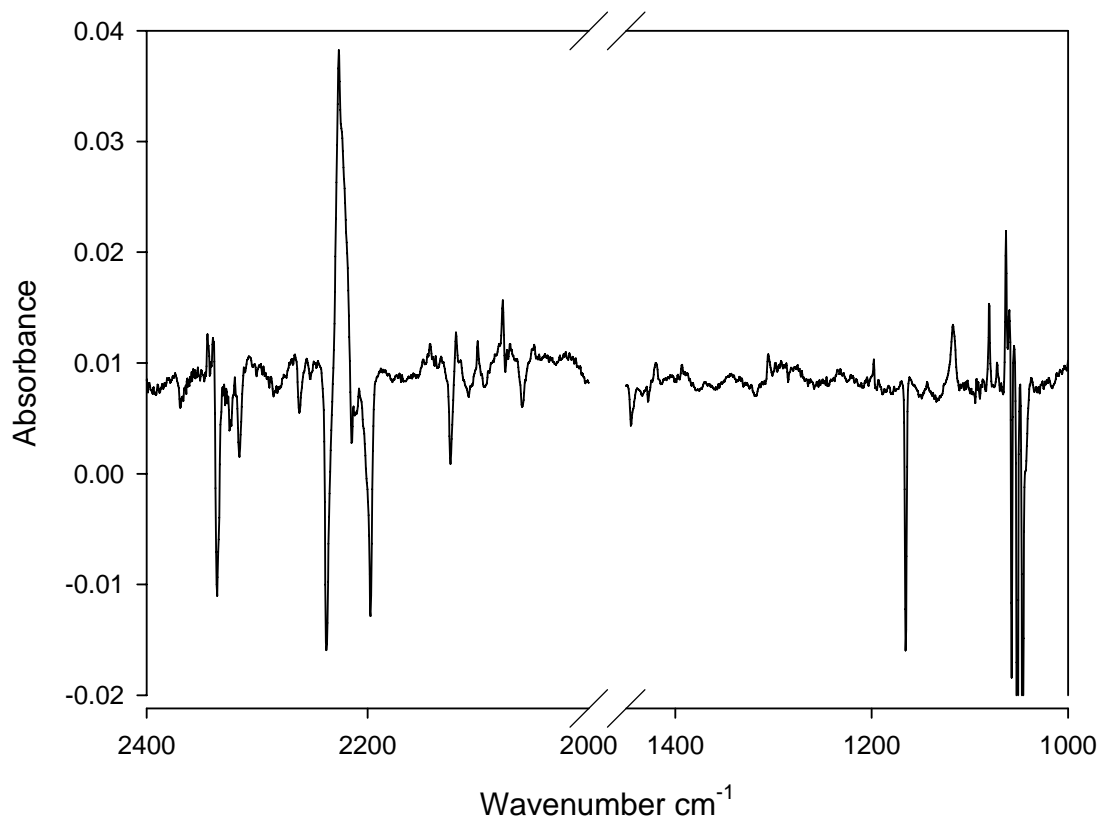


Figure 16: Portion of the resulting difference spectrum of the deposition of 1:100 C₃D₆. New features are present in the C-D stretching region (2300-2000 cm⁻¹) and in other regions corresponding with C₃D₈

Table 5: Wavenumber positions for the various products observed in the infrared spectra following reaction of V +1:100 C₃D₆:Ar. Wavenumbers are in cm⁻¹ units and blanks indicate unknown.

Experimental Wavenumber	Gas Phase C ₃ D ₈	Experimental Wavenumber	Gas Phase C ₃ D ₈
2345	CO2	1094	
2340	CO2	1080	1084
2319		1074	
2226	2225	1064	1064/1068
2212		1060.5	1068
2208		999	
2150	2148	993	
2145	CO/2144 obscured	883	
2139	CO	869	
2133	2135	863	
2120	2121	738	735
2100		684	688
2078	2080	638	
1420		604	
1305		572	
1246			
1198	1203		
1117			

While most of the features for C_3D_8 are observed in the experimental spectrum after deposition there are a few of the gas phase features which were unable to be detected: 2530, 2135, 960, 750 and 712 cm^{-1} were unobserved. Of these five features, all but 712 cm^{-1} were all listed as weak or very weak in the gas phase work. The lowered intensity of these features may be the reason why they are undetected in the present work. The feature at 712 cm^{-1} is a strong feature in both propene- d_6 and propane- d_8 , and the consumption of the feature in propene- d_6 obscures the appearance of this feature.

Several features other than C_3D_8 were also observed, some of which are known impurities. Features at 2345 and 2340 cm^{-1} are known to correspond to CO_2 , while 2140 and 2139 cm^{-1} correspond with CO along with a CO- H_2O complex, and 1305 cm^{-1} is known to be due to methane. With these impurities accounted for, there remain several features unidentified in the resulting spectrum after deposition. These features may correspond to the deuterated version of the additional product seen in the propene spectra. Table 6 shows the observed wavenumber positions for the unidentified features.

Table 6: Wavenumber positions for the unidentified product observed in the infrared spectra following reaction of V +1:100 C₃D₆:Ar. Wavenumbers are in cm⁻¹ units.

Experimental Wavenumber	Absorbance
2319	Weak
2212	Medium-Weak
2208	Medium-Weak
2100	Medium
1420	Medium (Broad)
1246	Very Weak
1117	Strong
1094	Weak
1072	Medium-Weak
638	Weak

4.3.2 Reaction of V with $C_3D_3H_3$

Several studies were conducted with different concentrations of 3,3,3 d_3 -propene, as this allows for the analysis of the features that appear on deposition. It was found that two groups of features appear in the spectra, which appear to be the isotopically substituted versions of propane and the additional product as they follow similar trends to those two products.

Also of note are the shared features in the resulting spectra after deposition for the different isotopomers. The feature at 1117 cm^{-1} is seen in both of the deuterated versions of propene, propene- d_6 and propene-3,3,3- d_3 and it is not seen in the non-deuterated version. While the feature at 1549 cm^{-1} in the propene sample is missing in the spectra of the d_6 and d_3 isotopomers. The feature at 1549 cm^{-1} is in the region for a V-H stretch while 1117 cm^{-1} is in accordance with a V-D stretch. Further analysis of these features is conducted in the discussion section and helps to identify the formation mechanism of the non-propane product.

Table 7: Wavenumber positions of observed features after deposition of several different concentrations of $C_3D_3H_3$ with V.

Wavenumber	1:50	1:100	1:200	Group Code
2964	i	d	d	a
2940	i	d	d/a	a
2908	i	d/a	d/a	a
2881	i	d	d/a	a
1475	d/a	i	i	b
1380	i	d/a	d/a	a
1296	i	d/a	d/a	a
1205	d/a	i	i	b
1117	i	i	i	b
1081	i	i	i	b
1028	i	d/a	d/a	a
1011	i	d/a	d/a	a
772	i	i	i	b
712	i	d	d/a	a
576	i	i	i	b
560	i	d/a	d/a	a

Note: Entries marked with “i” represent an increase or appearance of a feature in the particular experiment, while “d” represents a decrease compared to the previous concentration. The “d/a” represents that the feature did not appear. Group codes refer to the apparent group that the mode belongs to based on the trends it observes; “a” belonging to those similar to propane and “b” the additional product. Wavenumbers are in cm^{-1} units.

4.4 Reactivity of V + propene in the presence of water

Previous studies with ethene have shown the ability for hydrogenation of ethene at low concentrations in the presence of water.³ As the above results have shown hydrogenation of propene is also possible under low propene concentration conditions. The possibility that the hydrogenation source is water must be considered. As water has a constant trace presence in the apparatus, the possible reactions of the system water with C_3D_6 and reactions of D_2O and C_3H_6 were studied.

4.4.1 Reactions of H_2O with C_3D_6 and V

Under all previous studies water trapped in the system is seen to be consumed during deposition of metal atoms. By using deuterated propene it is possible to see if the reacted water atoms are the source for the hydrogenation, as new C-H modes should be seen in the infrared spectrum. Previously in section 4.3.1 propene- d_6 was studied and the results suggest that propene- d_8 was the major product in the high concentration study. In this section, both a high concentration and a low concentration were studied. Gas samples of 1:100 and 1:1000 propene- d_6 :Ar were condensed while depositing 3-5 cpm of vanadium for 1 hour. Additionally a sample of 1:400 d_6 -propene was studied using a higher metal flow at 7 cpm.

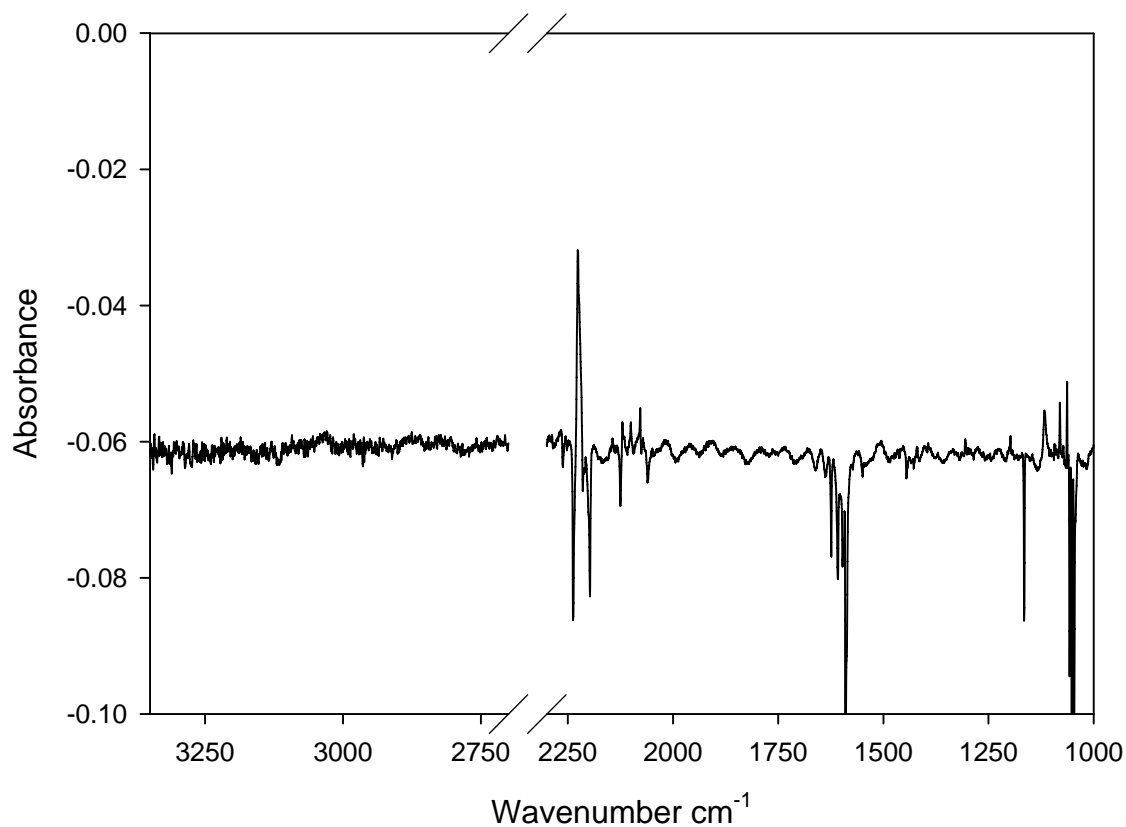


Figure 17: Comparison of the C-H stretching region (left of break) and the C-D stretching region along with majority of the rest of the spectrum (right of break) for the resulting difference spectrum of 1:100 propene-d₆:Ar after deposition with 3 cpm of vanadium.

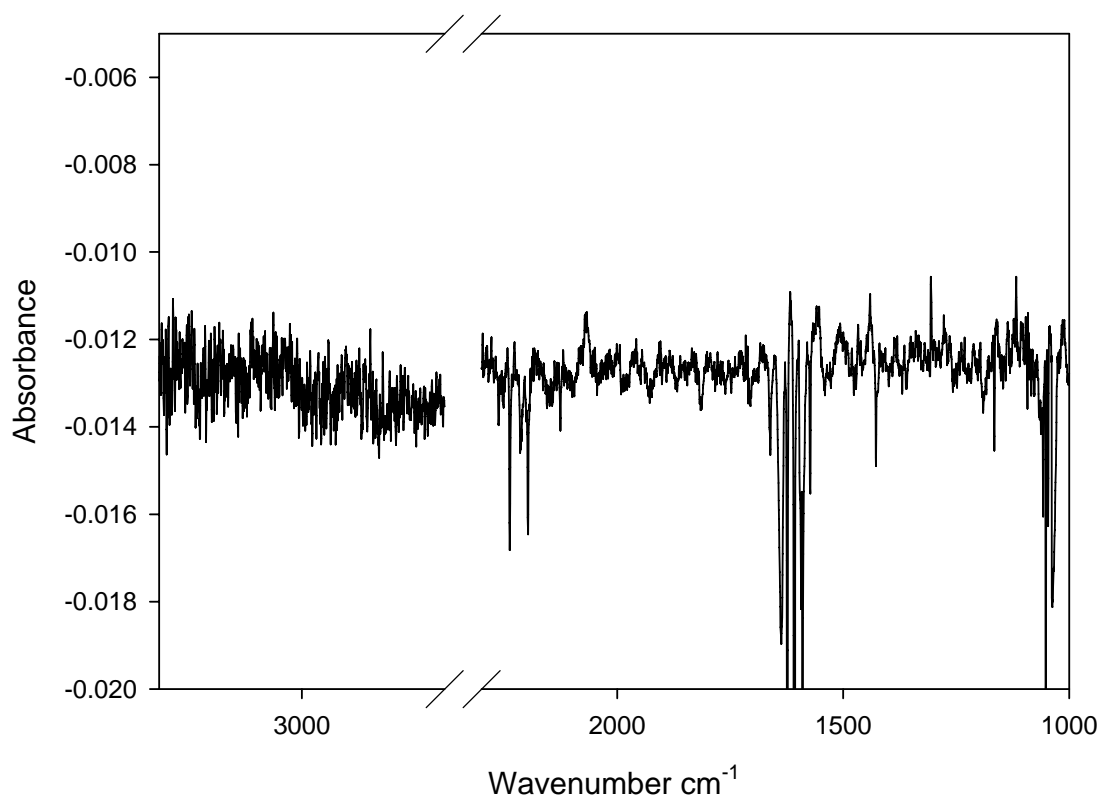


Figure 18: Comparison of the C-H stretching region (left of break) and the C-D stretching region along with majority of the rest of the spectrum (right of break) for the resulting difference spectrum of 1:1000 propene-d₆:Ar after deposition with 3 cpm of vanadium.

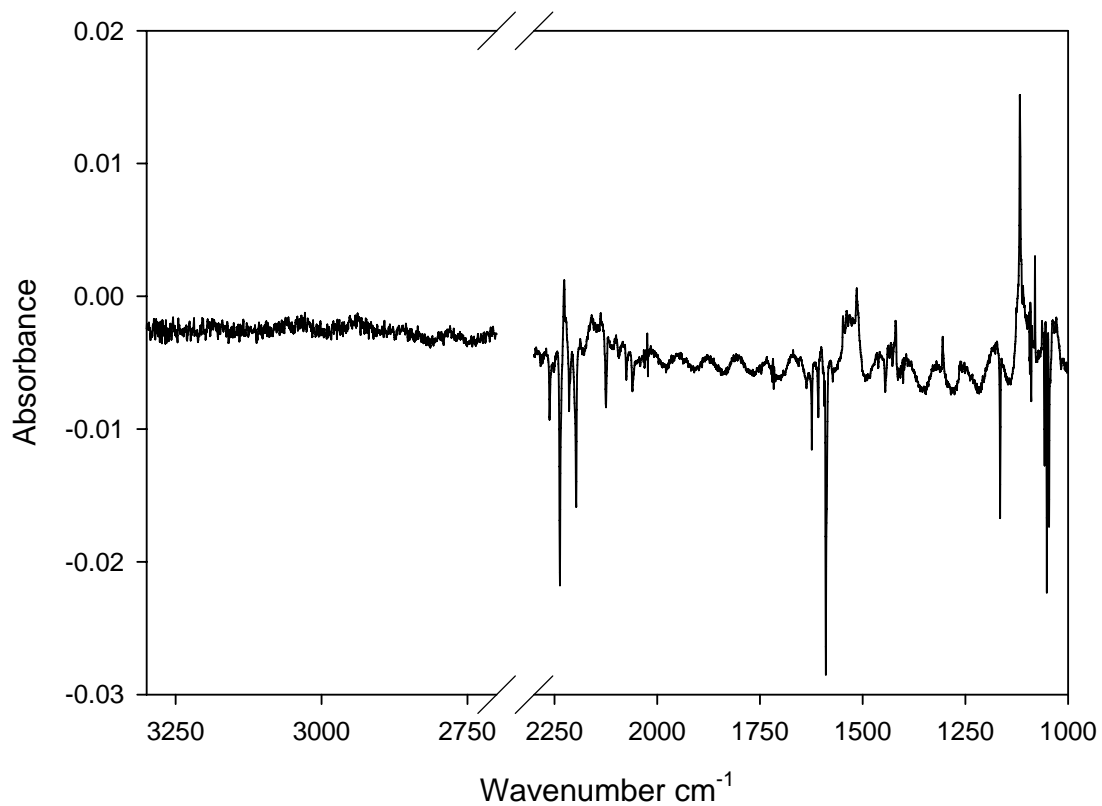


Figure 19: Comparison of the C-H stretching region (left of break) and the C-D stretching region along with majority of the rest of the spectrum (right of break) for the resulting difference spectrum of 1:400 propene-d₆:Ar after deposition with 7 cpm of vanadium.

It can be seen from Figures 17, 18 and 19 that while system water is consumed (negative feature at 1593 cm^{-1}) there is no incorporation of the hydrogen atoms into the propene- d_6 molecules, while there are signs of propane- d_8 formation.

4.4.2 Reactions of D_2O with C_3H_6 and V

In order to fully explore the possibility of water acting as the hydrogenation source of C_3H_6 , studies involving D_2O and propene were studied. Gas samples of 1:8:800 $\text{D}_2\text{O}:\text{C}_3\text{H}_6:\text{Ar}$ were prepared and deposited with 5 cpm of vanadium.

Figure 20 below shows that while D_2O is consumed (negative feature at 1175 cm^{-1}) there is no indication for incorporation of D into the propene molecules as the C-D stretching region (2350 to 2050 cm^{-1}) is quite bare other than the appearance of CO and CO_2 features. In other regions the familiar features of propane are present; 2970 , 2882 , 1472 , 1465 , 1180 , 1050 cm^{-1} , etc. The results of the study of the reactivity of water with propene and vanadium indicated that that under no conditions is hydrogenation caused by water incorporation, unlike the previous work with ethene.

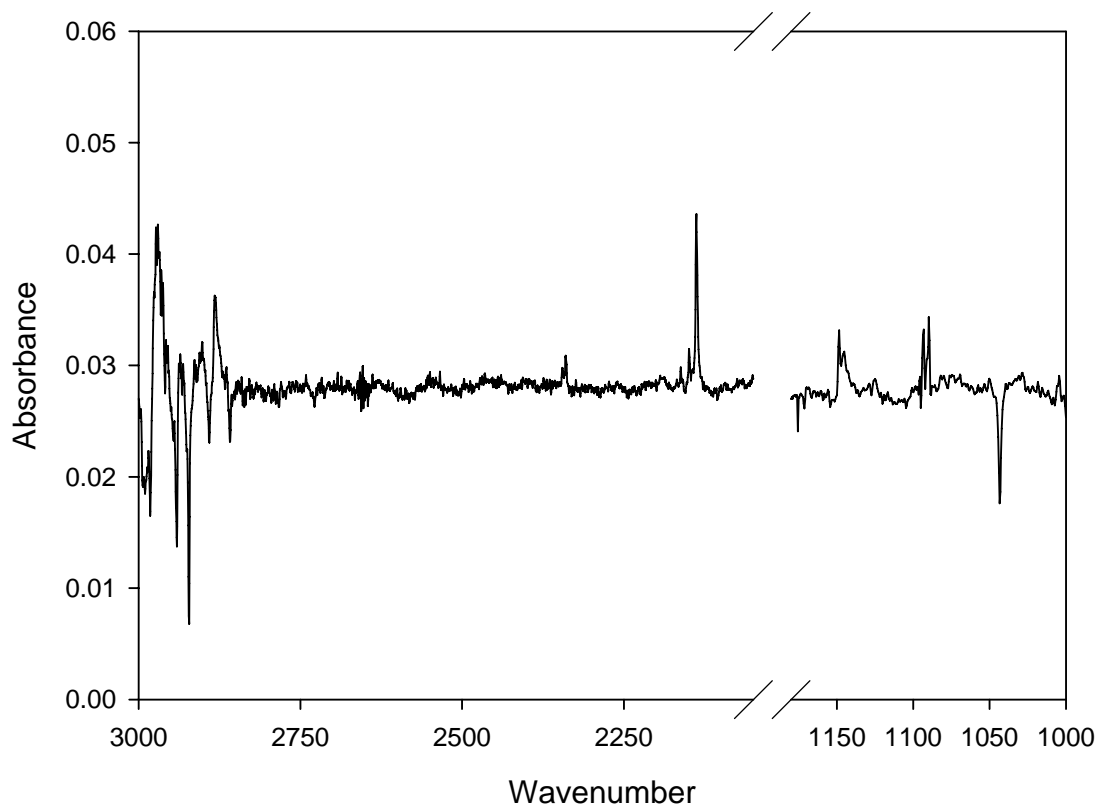


Figure 20: C-H and C-D stretching regions (left of break) and portions of the rest of the resulting difference spectrum after 1:100 propene:Ar with 1 torr D₂O deposited with 3-5 cpm V.

References for Chapter 4

¹ M.G.K. Thompson, PhD. Thesis, Queen's University, Kingston Ontario, 2007.

² Gough, K.M.; Baudais, F.L.; Casal, H.L.; *J. Chem. Phys.*, **1986**, 84, 549.

³ Thompson, M.G.K.; Parnis, J.M; *Inorg. Chem.*, **2008**, 47, 4045.

Chapter 5

Discussion

5.0 Propane production

From the initial investigation of the reactivity of vanadium with propene it can be seen that several new features are generated. The bulk of these new features seem to correspond to two species. It is quite evident that propane is formed upon condensation of propene with V. The generation of propane is confirmed by comparison with a 1:100 propane:Ar sample, which was condensed in the same apparatus. When comparing the two spectra it is easy to see the similarities in the features. All of the major features in the spectrum of propane are mirrored in the spectrum from the reaction of propene with vanadium. Most importantly, the relative intensities of each band are similar in both spectra. Features that appear in the propane:Ar spectrum that do not share similar intensity profiles to that of the propene vanadium spectrum are all caused by impurities. As the samples were created in separate glass bulbs, at separate times, and condensed at separate times they may have different levels of each impurity. For example in Figure 11 in the 1% propane spectrum there is a water feature that appears at 1593 cm^{-1} in the difference spectrum this is a negative feature, as water is consumed by the metal atoms that during condensation.

Further comparison of the two spectra shows that while propane is formed several other features are also apparent. Some of these features are known

impurities yet many are not and are proposed to be caused by the formation of a different product or intermediate.

Analysis of the series of experiments exploring the different experimental conditions show the production of propane is dependent on several conditions. The following section explores how these conditions effect the production of propane and how this helps to explain the mechanism of forming propane.

5.0.1 Production of propane- experimental conditions

The experimental conditions varied were propene concentration, propene:Ar gas flow, and metal flux. The variation of these experimental controls lead to a variation in the amount of propane formed. At high concentrations of propene it was found that propane production increased. The experimental results show that the concentration of 1:50 propene:Ar gave the largest amount of propane. The features of the other product formed, however, are seen to decrease as propene concentration increases, and aspects of this additional product are further discussed in section 5.1. This suggests that propane is the major product formed as production of propane dominates at high concentrations. The increasing amount of propane formed can be explained through the fact that at higher concentrations there is a higher likelihood of two propene molecules and a metal atom coming into contact before full condensation. It is likely that this reflects the fact that two or more propene molecules are needed in the process as one is needed to donate the hydrogen

atoms and one is needed to accept them. Similar results with high concentrations ethene have been found in the work of Thompson^{1,2}.

Analysis of the gas flow studies reveal that the increasing the gas flow causes an increase in the amount of propane formed. This increase appears even though the same amount of metal is used throughout the different gas flow rate experiments. This suggests that the higher flow rate increases the likelihood of reactivity with a metal atom throughout the deposition processes. This may be caused by increased diffusion throughout the matrix; as larger amounts of matrix material are used, the matrix warms slightly and the potential for reactivity of a propene molecule and metal atom may increase. It is also possible that the increase in flow will cause an increase in pressure within the reaction area. This may increase the likelihood of forming products as the probability for a reactive collision occurring will increase.

The results from the metal flux studies show that when a higher amount of metal is used, more propane is formed, similar to the concentration results. The study also shows that the increase in production of propane with increasing metal flux occurs both at high and low propene concentrations. These results suggest that at lower metal flux there are not enough metal atoms to react with the propene molecules. Thus increasing the metal flux increases the possible number of collisions with a propene molecule increasing the likelihood of reactivity. The amount of metal used is roughly on the order of 60 ng per minute at low flow (3 cpm) and 220 ng per minute at higher flow (11 cpm). At the higher

flow there is thus 220 ng of metal per 1 standard cubic centimeter of gas sample and at 1:100 propene:Ar this is roughly 1 vanadium atom for every 110 propene molecules. The fact that not all of the propene molecules can react with the vanadium atoms is quite evident in the spectrum, as after deposition, while some propene is consumed, the vast majority is left unreacted. The lowered reactivity at lower metal flux is further exacerbated by the fact that not every collision between propene and vanadium goes on to react to form propane. The fact that a second propene molecule is needed to produce propane has already been discussed. Along with this, the gas phase kinetic data suggest that vanadium will only insert into propene in about 1 in every 30-50 collisions for the ground state. The excited state metal atom is more reactive, reacting in about one in every 2 collisions.^{3,}

While increasing the metal flux does increase the propane formation it is not possible to continue to use ever increasing amounts of metal. This is because at higher metal flux the lifetime of the metal filament is reduced significantly. The increased temperature, along with the rapid heating and cooling of the filament, causes it to become unstable and break at the centre. Additionally at higher metal flows it become increasingly difficult to control the flux of metal from minute to minute as the resistance changes along the filament throughout the experiment. For these reasons the metal flux was held at 3-5 cpm throughout the majority of the other experiments.

5.0.2 Effect of irradiation and comparison with ethene

To investigate any possible photoinduced chemical processes with vanadium and propene, matrices formed containing V and propene in Ar were exposed to irradiation from a UV-Vis lamp. The energy from the light can be absorbed by the metal atom through an electronic excitation. This excess energy can then be used by a molecule containing a metal atom to overcome barriers to formation if it is trapped in a small potential energy well. Irradiation of the matrices containing V atoms in pure Ar with > 455 nm light has previously shown to cause no major consumption of V atoms nor to cause formation of any products.¹ In the present work further irradiation of the matrices at all wavelengths investigated showed no formation of any new infrared active molecules. This result is in stark contrast to the results found previously with ethene where significant changes were seen after irradiation of an ethene:Ar matrix condensed with vanadium under similar conditions (1:100 ethene:Ar 3 cpm V).¹ The effect of irradiation on propene:Ar with V is the first major difference seen between the propene- and ethene-vanadium systems.

Analysis of the gas phase rate constants for the reactions of vanadium with propene and ethene along with the bond energies involved in each reaction give some light into why this difference occurs. Gas phase kinetic data from both Senba³ and Ritter⁴ suggest that while ground state vanadium metal atoms do not react with ethene, insertion into propene is quite possible. The excited state data also shows that while excited state vanadium does insert into ethene, it is

between two and three times faster towards the insertion into propene. This suggests that in the case of propene matrix isolation studies the metal atoms can react with propene even when they are not in an excited electronic state. In the case of the ethene system metal atoms excitation is necessary for the formation of ethane. Many of the metal atoms will be excited from the light emitted from the metal filament, however some ground state metal atoms remain and are condensed in close proximity to an ethene molecule. When irradiation of the matrix occurs the metal atoms become excited and may react with an ethene molecule in close proximity. In the case of propene, however, the excited state metal atoms seem to react on nearly every collision with a propene molecule, lowering the likelihood of finding a non-reacted excited state metal atom. Along with this, the ground state metal atoms are found to react with propene molecules and thus if they were condensed in proximity with a propene molecule they may react without the need for excitation. Thus the increased reactivity of both the ground state and excited state vanadium atoms towards propene may cause a decrease in further photochemical reactions after condensation.

The reason for this apparent increase in reactivity of vanadium atoms is most likely due to the lowered bond energies of the methyl hydrogen atoms in propene compared to that of ethene. When looking at the bond dissociation energies of removal of one of the hydrogen atoms in ethene, all C-H bonds are equivalent and correspond to a dissociation energy of 419.5 kJ/mol.⁵ In propene, however, there are several distinct C-H bonds, and of these the C-H bond of any of the equivalent methyl hydrogen atoms have the lowest bond dissociation

energy at 361.1 kJ/mol.⁵ It is easy to see that the required energy needed for the vanadium atom to insert into the C-H bond of propene is lower than that needed for ethene. It is because of the extra energy needed in the case of ethene that the ground state metal atom does not seem to react with ethene. This barrier is lower in propene and appears to be low enough to allow for the metal atom to insert.

5.0.3 Isotopic substitution of H analysis

The study of isotopically substituted homologs of propene used in this study have been conducted with propene-d⁶ and propene-3,3,3-d³. A separate study monitoring the reactivity of D₂O with propene and V was also conducted and is discussed further in section 5.2. The majority of the experiments conducted with propene-3,3,3-d³ are of direct relevance to the analysis of the additional product and that majority of its analysis is conducted in that section.

The theory behind using isotopically substituted homologs as a method for better understanding the structure and mechanism of particular compounds has been explained previously in the first chapter. Using propene-d⁶ helps to ascertain two main facts under question. First, as the only source of D in the system, any evidence for D addition into propene shows that the hydrogenation source must in fact be another propene molecule. Additionally, it adds further confirmation of the production of propane, as the absorptions for gas phase propane-d⁸ are known. Table 5 in the results section shows that many of the

matrix isolated infrared absorptions correspond well with the gas phase infrared spectrum of propane-d⁸ reported by Gough.⁶ This gives further evidence that propane is indeed formed in the condensation of propene with vanadium. Additionally the lack of any apparent C-H stretches in the spectrum suggests that propene is the only source of hydrogenation at this concentration. Possible water hydrogenation at lower concentrations of propene is analyzed in section 5.2.

Results of the reaction of propene-3,3,3-d³ with V, with respect to the propane production, focused on determining which hydrogen atoms were involved in the process. It is evident that new C-H modes in the methyl region appear in the spectrum after deposition. This suggests that at least one of the atoms transferred from the propene come from the non-deuterated side. Additionally in the region corresponding to a CH₂ twist the expected feature at 1257 cm⁻¹ is absent. Similarly, a feature at roughly 1467 cm⁻¹ should appear however again this is absent. There is, however, a shifted feature at 1295 cm⁻¹ along with a feature at 790 cm⁻¹ because of the absence of either pure CH₂ or CD₂ motions it is possible that the features that are seen are due to a CHD twist. This would suggest that the first hydrogenation location originates from the methyl group as this is the only site where D is available.

As it has been shown that propane is indeed formed in the reaction of vanadium atoms and propene, the exploration of the mechanism used to form this product is the next logical step. Before a full mechanistic analysis of the formation of propane is possible the results from the additional product must be

completed in order to determine if it is formed in the process of propane formation and is in fact an intermediate. Analysis of this product will give valuable information about the mechanism of propane formation.

5.1 The additional/intermediate product

From the analysis of the initial study of the reactivity of vanadium atoms with propene it was found that several other features that could not be explained by impurities were apparent along with propane. It also appeared that many of these features seem to track together during the changing of conditions, and this lead to the suspicion that they may be due to an additional product or an intermediate along the reaction pathway towards the hydrogenation of propene. These absorption features seem to correspond with some sort of organometallic molecule. In order to determine the nature and structure of this molecule several studies were performed. Initially the study revolved around how the features change upon altering the experimental conditions in a similar manner to the study of propene. After this, isotopic studies were performed in order to gain a better understanding of the structure of the molecule.

5.1.1 Production of the additional product- experimental conditions

As in the study of conditions with respect to propane production, the experimental conditions explored were propene concentration, propene:Ar gas flow, and metal flux. As mentioned earlier, at high concentration of propene it was found that the additional product production decreased. The experimental results show that the concentration of 1:1000 propene:Ar gave the largest amount of the non propane features. This response, which is opposite to that

found with propane, indicates that this product may in fact be a molecule which acts as an intermediate in the process of forming propane. If the formation of this product is caused by metal reaction with one of the propene molecules before a second can react with it and go on to form propane, this may explain why it is observed most frequently at lower concentrations. At high concentrations, once the intermediate is formed it quickly goes on to react and form propane.

However, at low concentrations the likelihood of a second propene molecule being at an appropriate location for further reactivity is lowered. This causes a build up of the intermediate product as it can not complete the hydrogenation reaction without a second propene molecule. When comparing this result with the previous work completed with ethene it appears to fit well, as the first step in hydrogenation is the reported insertion into the C-H bond of ethene. The insertion intermediate molecule in the ethene work is also seen to maximize at lower concentrations of ethene. Additionally, in the case of propene it appears that the maximization of the additional product does not go on indefinitely as propene concentration is lowered. Figure 13 shows that the increase in appearance of the additional product begins to tail off around the 1:1000 propene:Ar concentration. This effect also agrees with the idea that it may be the primary product, which acts as an intermediate in the formation of propane; as at even lower concentrations the likelihood of a vanadium atom inserting into a propene, molecule begins to lower as there are fewer and fewer propene molecules available.

Analysis of the flow rate experiments show similar results to that found with the propane production study. Again, a higher amount of the product is formed at higher gas flow rates. This is again thought to occur through either an increase in diffusion or an increase in the pressure at the reaction area. The flow rate study also shows a confirmation that all the features observed are in fact most likely due to the same product species, as the features all respond to increased flow in similar ways.

Figure 15 shows that similar to the results found for propane the amount of the additional product increases upon increasing metal flux. The reason for this increase in formation of the product is caused by a similar situation found with propane. The increasing amount of metal increases the potential for a metal atom to insert into a propene molecule, such that more of the product can be formed. As the metal flux is the only thing that changes (the propene concentration remains the same), the likelihood of two propene molecules being in the same location does not increase. As such, the product again builds up and does not further react to make propane. It should be noted that there should be a slight increase in the probability that two propene molecules and a metal atom will be in proximity to form propane at higher metal flows. This is because while at low metal flux there is a small chance that there will be two propene molecules that could react together if there was a metal atom available, however due to the lower metal flux they can not react. Increasing the metal flux increases the probability that there will be a metal atom available for these two propene molecules to react with. This would act as a decreasing factor towards

intermediate formation however this effect is very small at the low concentrations used. Additionally, as with the flow rate experiments the metal flux results again show that the reported peaks for the intermediate product are most likely caused by the same molecule.

5.1.2 Structural analysis of infrared results

From the analysis of the condition variation experiments, many of the non-propane features that appear in the spectrum after deposition of propene with vanadium can be attributed to an intermediate product. Using a group frequency approach these features can be used as an initial guide into interpreting the structure of this intermediate. Analysis of the spectra throughout the concentration studies leave these several features corresponding with the intermediate product 1549, 1480, 1207, 975, 810, and 728 cm^{-1} . The feature at 1549 cm^{-1} appears to be quite strong in the IR spectrum and this feature is located in a region of the IR suggesting it belongs to some sort of vanadium hydride stretch. Direct determination of the other features is not possible as many of the features may correspond to more than one type of mode. By using the fact that it is known that these features must be formed with only three possible atoms, C, H and V, it is possible to narrow down the possibilities for these features. Figure 21 shows two possible structures that may lead to the appearance of these absorptions, Table 8 below indicates what motion of the molecules correspond to each absorption.

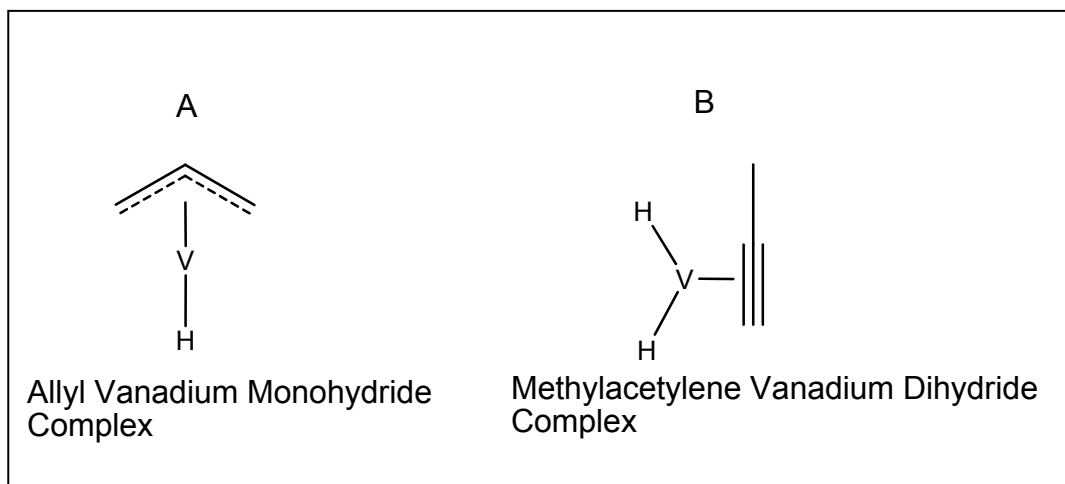


Figure 21: The two possible structures for the intermediate product based on their infrared absorptions. Note that the bond between the vanadium and the allyl is a coordination bond between the metal atom and the whole complex, not just the one carbon atom.

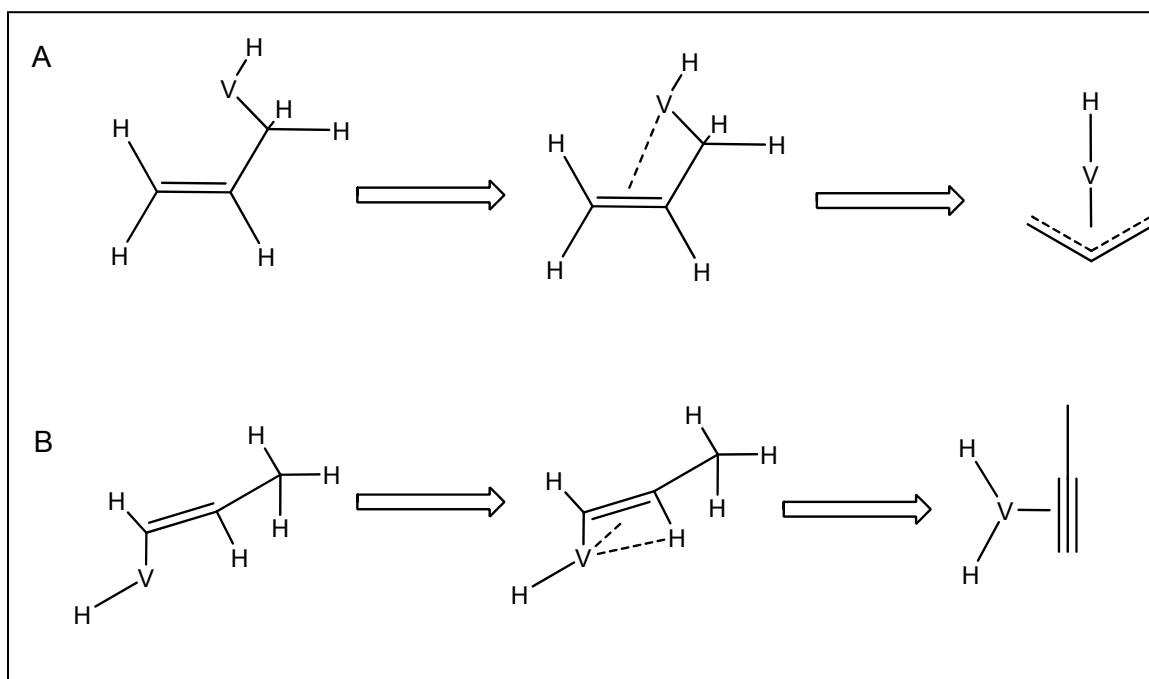
Table 8: Positions of new bands of a metal containing species on deposition of propene with metal, with possible assignments for two suspected intermediate structures.

Wavenumber (cm^{-1})	Allyl monohydride species	Dihydride acetylene species
1549.6	V-H	V-H
1480	CH_2 scissor	CH_3 deform
1207	Unknown	CC triple bond mode
975	CH allyl	Unknown
810	CH_2 wag	Unknown
728	allyl ring mode	V--CH bend

As the initial analysis of the infrared features has shown that there may in fact be two possible structures corresponding to these absorptions it is important to see if either of these two structures can actually form directly from reaction of propene and vanadium. A third structure the initial insertion product in the formation of the methyl acetylene complex which could be formed was ruled out as no evidence for a C-C double bond stretch was apparent. The allyl structure can be formed through initial coordination of the double bond of propene followed by insertion into any of the C-H bonds located on the methyl group. The metal hydride then moves slightly towards the attractive double bond, this process is believed to be barrier-less. As this is occurring the hydrocarbon becomes stabilized in the allyl confirmation with the metal atom complexed in the centre. If, instead, the vanadium atom inserts into the C-H bond of the CH_2 group, the metal hydride may be attracted towards the double bond and abstract the hydrogen atom located between the methyl and the double bond. This would

leave a methylacetylene group and a vanadium dihydride. Scheme 1 below illustrates both of these two mechanisms.

Scheme 1: Intermediate complex mechanisms A) the allyl product and B) the methylacetylene product



The two proposed schemes suggest that it is in fact possible for the formation of either of these two compounds. Consequently, further analysis is needed to identify which of the two molecules is the source of the observed absorbances. It can be hypothesized that the allyl is the most likely structure of the two to be formed, as the C-H insertion into the methyl group is more highly favored than the others thermodynamically. As indicated earlier, the bond dissociation energy for the breaking of the C-H bond of the methyl group is 361.1 kJ/mol, which is

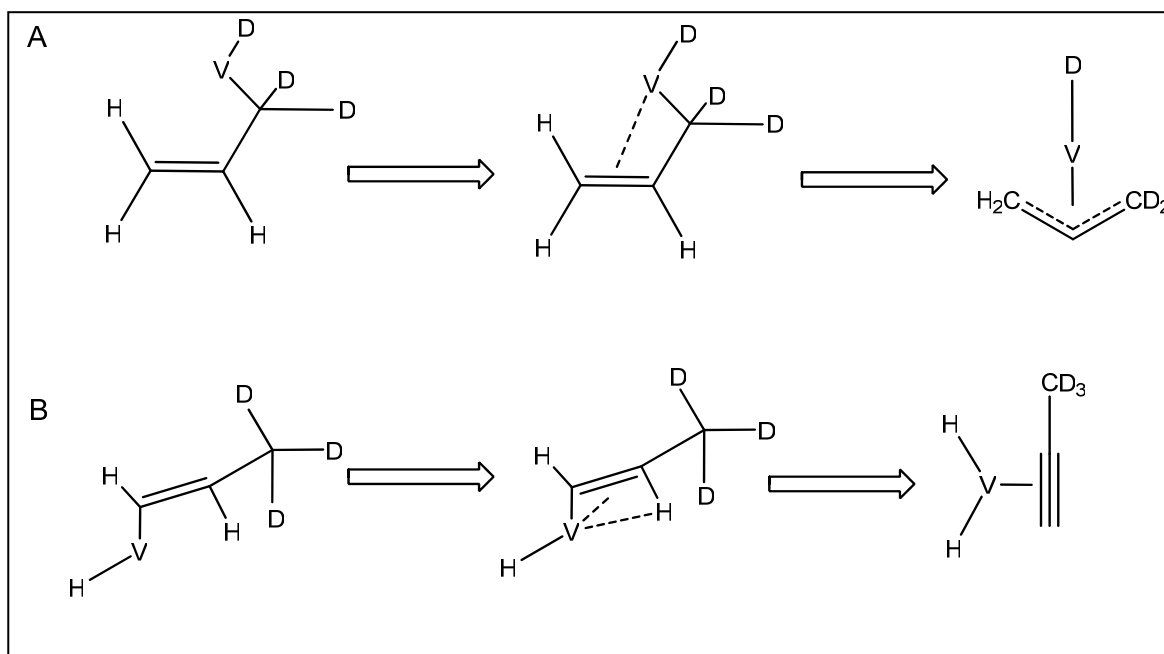
lower than all other C-H bonds in propene. In order to further research the structure of the intermediate, isotopic homologs were explored.

5.1.3 Structural analysis - Isotopic study

Using isotopic homologs of propene it is possible to further explore the structure of the intermediate product. Using the partially deuterated propene-3,3,3-d³ it is possible to identify where in the molecule the vanadium atom inserts. Additionally, comparison of the observed bands in the three isotopic homologs (propene, propene-d⁶, and propene-3,3,3-d³) it is possible to see which features are common between the three sets, which also helps in identification. These two methods allow for a reasonably definitive assignment of the structure of the intermediate product.

As the two proposed mechanisms for formation of the intermediate have different insertion locations on the propene molecule, the use of propene-3,3,3-d³ allows one to determine if either, both or possibly neither are formed. They can be identified because the insertion point leads to the specific type of hydride found. In the allyl case the hydrogen from the methyl group forms the hydride, whereas in the case of the methylacetylene complex, the hydrogen atoms from the CH₂ and CH group form the dihydride. In propene-3,3,3-d³ the methyl hydrogen atoms have been substituted with D atoms, and this will leave a V-D group if the allyl is formed or leave the VH₂ group if the methylacetylene complex is formed. Scheme 2 below illustrates these two possibilities below.

Scheme 2: The mechanisms illustrating the formations of the two possible structures for the primary product using propene-3,3,3-d³.



In the introductory section of this work (Chapter 1) the effect of an isotopic substitution between a hydrogen and deuterium atom on the location of a X-H stretch was explained. The observed shift from the V-H to V-D is expected to be roughly equal to a factor of $\sqrt{2}$. In the unaltered version the product is known to have a V-H stretch at 1549 cm^{-1} and this would indicate that the expected V-D stretch should lie between $1090\text{--}1150\text{ cm}^{-1}$. There is a range of values, as the isotopic shifts may not be exactly equal to root 2, as noted previously. Scheme 2 illustrates that if the allyl complex is formed, a band occurring in the V-D range is expected, while if the methylacetylene complex is formed no V-D band should be

seen and instead a V-H mode should be seen in a similar location seen in the undeuterated version. If both V-D and V-H modes are observed it may be evidence that both structures are formed.

Analysis of the difference spectra for several concentrations of propene-3,3,3-d³ in argon is summarized in Table 7. In this table it is apparent that there is a feature at 1117 cm⁻¹ which is in the region expected for a V-D stretch. It is also seen that there is no feature around 1550 cm⁻¹, which would be expected with a V-H stretch. Evidence for a V-D stretch and lack of a V-H stretch suggests that only the allyl complex is formed. This result is in accord with the analysis of the bond dissociation energies for the propene molecule, as the most likely location for insertion should be the methyl hydrogen.

When the results from the propene-d⁶ studies are taken into account it is apparent that the feature at 1117 cm⁻¹ remains. The fact that this feature does not shift between the d³ and d⁶ isotopomers suggests that the mode that causes this feature is in a location that does not change between the two isotopomers and is isolated from the rest of the molecule, as there is no shift. Additionally the feature does not appear in any of the spectra for the undeuterated reactions, this suggests that it is neither an impurity nor caused by the back bone structure of the intermediate. For these reasons it is reasonable to claim that this feature is caused by the V-D stretch and that there is no V-H moiety formed. These results indicate that the allyl structure is the most likely structure for the intermediate and that there is no evidence for the methylacetylene structure as the intermediate.

5.2 Water reactions

In order to fully explore the hydrogenation mechanism of propene it is important to explore all possible H sources that are found in the matrix isolation experiments. Other than propene itself, water is the only other major source of hydrogen in the apparatus. The presence of water as a trace impurity in the system is found in all experiments and is found to vary from one experiment to the next. It has been shown that water was a possible hydrogenation source in experiments conducted with ethene previously.² Thompson et al. conducted several experiments using heavy water (D_2O) with regular ethene and experiments involving H_2O reacting with C_2D_4 . Results from this study showed that at low concentrations of ethene to Ar the hydrogenation source of ethene was in fact water, found within the system.

In order to investigate whether a similar process occurs in the case of propene, similar experiments were conducted investigating both a $H_2O:C_3D_6$ system and a $D_2O:C_3H_6$ system. If new C-H modes are apparent in the C_3D_6 spectrum after deposition or if new C-D modes are apparent in the C_3H_6 spectrum then water must be the source of the hydrogenation as it is the only source of H or D, respectively.

The original study using C_3D_6 shown in Table 5 shows no evidence for water incorporation and evidence for C_3D_8 is seen, and a subtraction spectrum of this is shown in Figure 17. This study was conducted at high propene

concentration (1:100 propene:Ar) in order to investigate the process under conditions similar to the ethene study. Lower concentration studies using 1:1000 propene were also conducted. Figure 18 shows the difference spectrum of 1:1000 C₃D₆:Ar, the C-H region is shown along with much of the rest of the spectrum. It can be seen that in the C-H stretching region between 3300 and 2700 cm⁻¹, there is no evidence for any new features. When compared to the C-D region the difference is quite obvious with a large number of features found between 2250 to 2000 cm⁻¹. It is also important to note that there are indeed signs of water consumption, as the negative feature at 1598 cm⁻¹ shows that the metal atoms do react with the water. However, they do not go on further to react with propene or the intermediate.

In order to be sure of the fact that water is not the source of the hydrogenation of propene under these conditions further experiments were conducted with 1:100 C₃H₆:Ar and D₂O. Before conducting the experiment the system was exposed to a large amount of D₂O vapour, which allowed for exchange of any H₂O found in the system, in order to leave the system essentially H free. This study confirmed that no water is incorporated into propene, as evidenced by the lack of new C-D modes in the spectrum. The spectrum is shown in Figure 20. The modes in the 2300-2000 cm⁻¹ range are attributed to CO₂ and CO. Additionally, evidence for new C-H modes which correspond to propene are quite prominent in the C-H region. It should also be pointed out that the observations by Thompson showed that under low concentrations of ethene a fairly substantial amount of ethane was produced.

This can not be said to be the case for the propene study, as when higher concentrations of propene are used much more propane is formed than under low concentration. The residual propene that is formed at the low concentration may be caused by the higher reactivity of propene compared to ethene.

These results suggest that unlike when low concentrations of ethene are deposited with vanadium, water is unable to incorporate into the propene molecule or the intermediate. It is important to note that the water present in the system is consumed by the metal atoms, however they do not react with propene. It is known that vanadium atoms can insert into water which then can further go on to dissociate leaving molecular hydrogen (H_2) and VO, as discussed in Chapter 2. It is thought that this is the process that is consuming the water molecules. This would leave a reactive VO species; however, there is no evidence of this molecule being the source of any reactivity and no sign that an intermediate involving a VO species is present.

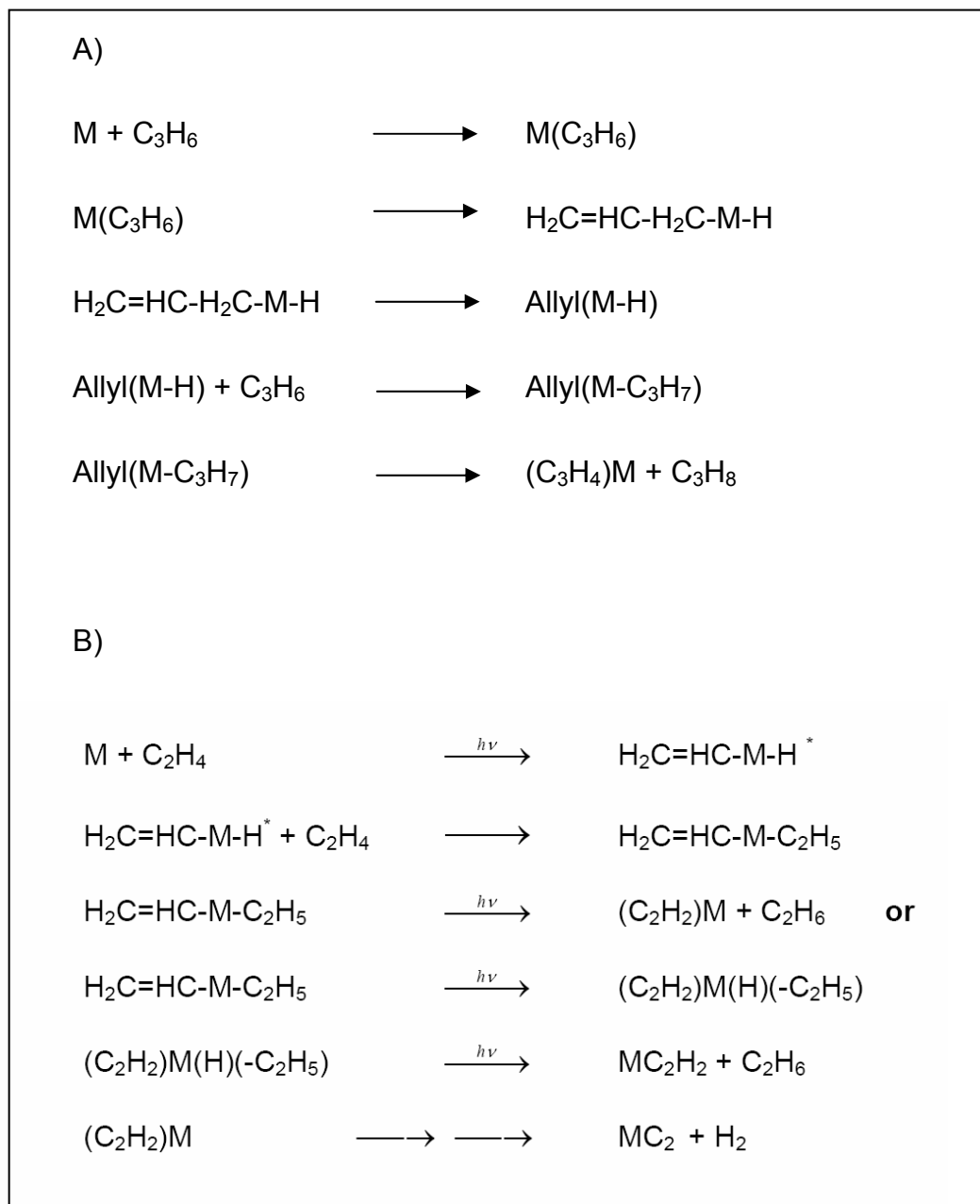
The difference in the ability to use water as the hydrogenation source between ethene and propene is interesting. It is most likely that it is again caused by the difference in the reactivity of the two alkenes towards the ground state metal atom and the general increase in reactivity of the methyl hydrogen. Results from Kauffman et al.⁷ show that the energies involved in the formation of a water adduct followed by metal atom insertion lead to a exothermic process of 230 kJ/mol, suggesting that the while the rate constant for this process should be slightly better than it is towards for propene, it should not be all that dissimilar.

In the case of ethene none of the ground state metal atoms can insert into ethene. Such atoms will likely instead react with a water molecule, should they encounter one. As both the excited and ground state metal atoms may insert into propene and as the rate of the reaction for the excited state towards propene is higher than it is towards ethene, there is a higher probability for propene-propene interactions than propene-water. The rapid formation of the intermediate product lowers the ability to form the water insertion product, with enough time to react with unreacted propene. This lowers the likelihood of hydrogenation of propene caused by water.

5.3 Formation of propane mechanism

With the identification of an intermediate and with water ruled out as a potential hydrogenation source it is possible to investigate the mechanism in which propane is formed. From the analysis above, several key aspects of the mechanism have been determined. First, it is evident from the water and isotopic studies that propene is the source of hydrogenation through a two propene mechanism. Second, the mechanism moves through an intermediate which can be isolated and is most likely of the form of an allyl metal hydride complex. Finally, the isotopic studies show that the first insertion step is into one of the methyl hydrogen atoms and it is this hydrogen which is the first to insert into the second propene molecule. Additionally, previous gas phase studies showed that there was no observable kinetic isotope effect found in the reactions of vanadium and propene. The lack of a kinetic isotope effect suggests that the first step in the reaction is coordination of the metal atom with the double bond of propene which is then followed by insertion. If direct insertion into the C-H bond occurred, then a kinetic isotope effect would be expected to occur as the rate between C-H and C-D insertion should be different. Scheme 3 below, along with Figure 22, illustrates the proposed mechanism from metal coordination through the formation of propane.

Scheme 3: Reaction mechanism for production of propane from propene hydrogenation with vanadium metal atoms, "A". Additionally the reaction mechanism for the similar process found for ethene reported by Thompson is used for comparison¹ "B".



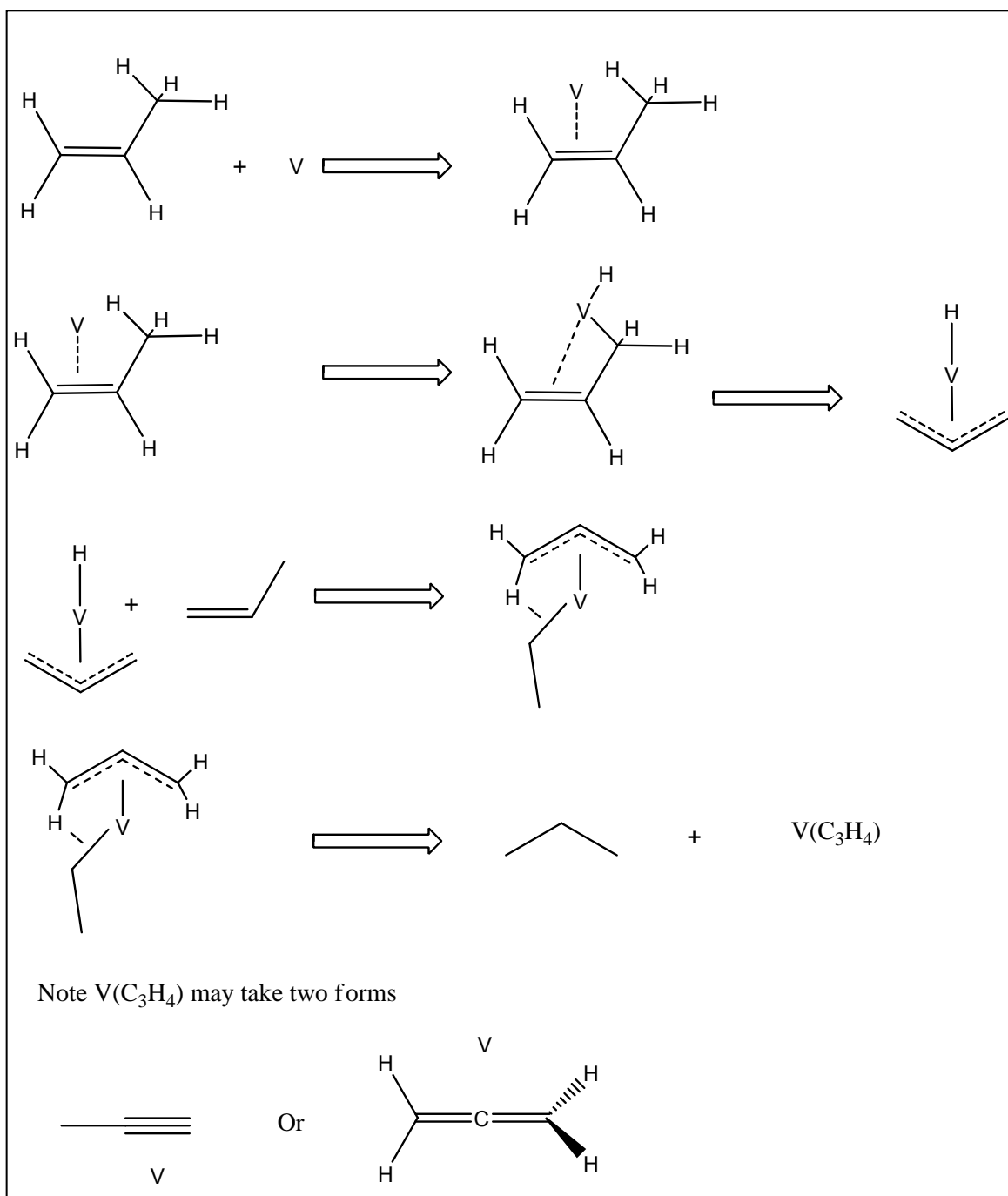


Figure 22: Structural representation of the possible reaction mechanism for the formation of propane from propene hydrogenation with vanadium metal atoms.

The proposed mechanism for the formation of propane through sacrificial hydrogenation of propene follows the similar process that was seen to cause the hydrogenation of ethene. All observed features fit well with the proposed mechanism and no features observed contradict it. Additionally the formation of the allyl intermediate and the ability for vanadium metal to cause H₂ removal fit well with known studies of propene. The allyl intermediate seems to be a stable enough intermediate to be trapped in an argon matrix and insertion into the methyl hydrogen of propene is the most likely insertion position. The ability for transition metal atoms V and Zr⁸ to remove H₂ has been previously seen in gas phase work; however, this appears to be the first sign that the H atoms can be transferred to another propene molecule.

There is one aspect of the proposed mechanism which the experimental evidence do not confirm, however. Along with propane as the major product a additional species should be formed which is either a metal-hydrocarbon complex or a hydrocarbon with the metal atom separated from it. The propene molecule from which the hydrogen atoms originate must be left over after the reaction. The removal of these two hydrogen atoms will leave a C₃H₄ fragment and this structure may take up two possible forms. From the proposed mechanism a methylacetylene product is most likely formed after the second hydrogen is from the terminal carbon of the allyl group. It is also possible that the fragment will take up the form of allene, however this would either involve abstraction of the hydrogen from the centre carbon in allyl or fast rearrangement from the methylacetylene structure formed after removal of the terminal

hydrogen. Both of these structures have infrared absorptions which should be visible in the spectrum after deposition. Additionally these features should track similar to that of propane as it should be formed in the same process. Analysis of all of the produced spectra, however, show no evidence for any additional product formed along side propane. Features which were could possibly correspond to a methylacetylene product were seen in the investigation of the intermediate; however, they were attributed to the allyl intermediate as they do not track with propane and the isotopic study showed they were more likely caused by an allyl complex.

While the lack of this product is troubling, similar results were observed in the study of ethene by Thompson. The lack of evidence for a MC_2H_2 product was explained by the possibility that this product quickly decomposes into MC_2 and H_2 , as H_2 is a linear diatomic and is unobservable in the IR spectrum due to symmetry. The lack of evidence for the formation of the metal carbide species is supported by a study conducted by Kafafi. In this work iron atoms were used and they also propose the formation of a metal carbide species which as not observed.⁹ It may be the case that a similar process forming MC_3 and $2H_2$ occurs in the reaction that occurs with propene. This is supported by the work of Song et al. where they show that the gas phase V atom may cause full dehydrogenation of propene,¹⁰ and this is shown in equation 2.1 in Chapter 2.

As the proposed mechanism fits the observations and follows the expected processes based on past research conducted with gas phase propene

studies and past matrix isolation studies with ethene, the proposed mechanism is thought to be in agreement with all known aspects of the reaction. The lack of evidence for additional products along side propane is similar to results found for ethene by both Thompson and Kafafi. It is believed that it may be possible that this is due to the fast decomposition into a metal carbide and 2H_2 .

References of Chapter 5

- ¹ M.G.K. Thompson, PhD. Thesis, Queen's University, Kingston Ontario, 2007.
- ² Thompson, M.G.K.; Parnis, J.M; *Inorg. Chem.*, **2008**, 47, 4045.
- ³ Senba, K.; Matsui, R.; Honma, K.; *J. Phys. Chem.*, **1995**, 99, 13992.
- ⁴ Ritter, D.; Carroll, J.J.; Weisshaar, J.C.; *J. Phys. Chem.*, **1992**, 96, 10636.
- ⁵ Weast, R.C.; Lide, D.R.; *CRC Handbook*, 70th ed. **1990**, CRC Press, Inc. USA.
- ⁶ Gough, K.M.; Baudais, F.L.; Casal, H.L.; *J. Chem. Phys.*, **1986**, 84, 549.
- ⁷ Kauffman, J. W.; Hauge, R.H.; Margrave, J.L.; *J. Phys. Chem.*, **1985**, 89, 3547.
- ⁸ Wen, Y.; Porembski, M.; Ferrett, T.A.; Weisshaar, J.C.; *J. Phys. Chem. A*, **1998**, 102 8362.
- ⁹ Kafafi, Z.H.; Hauge, R.H.; Margrave, J.L.; *J. Am. Chem. Soc.*, **1985**, 107, 7550.
- ¹⁰ Song, L.; Freitas, J.E.; El-Sayed, M. A.; *J. Phys. Chem.*, **1990**, 94, 1604.

Chapter 6

Summary

6.0 Summary

Vanadium metal atoms generated through a resistively heated metal filament have been shown to insert into the C-H bond of propene. This forms a product identified as the allyl metal hydride which has been shown to further react with a second propene molecule leading to sacrificial hydrogenation forming propane.

The mechanism for propane formation is proposed to occur through metal coordination with the π bond of propene, followed by metal insertion into one of the C-H bonds of the methyl group. This then forms the allyl metal hydride. Subsequently, a second propene molecule inserts into the M-H bond followed by removal of the second hydrogen from the terminal hydrogen of the allyl group. Elimination of propane then occurs leaving a $V(C_3H_4)$ group. No evidence is found for a $V(C_3H_4)$ group and it is believed that this species goes on to form a VC_3 group and $2H_2$. This is supported by previous gas phase propene results along with previous work conducted with ethene in a matrix isolation study.

Comparison with previous work with ethene reveals that the addition of the methyl group changes some aspects of the chemistry between the two species. Propene has shown higher reactivity towards vanadium in the gas phase and this has been reflected in this work in the differences found following irradiation and the apparent lack of reactivity towards water. The products formed on deposition of vanadium with propene showed no reactivity towards irradiation or water in

stark contrast with the results found with ethene. This is proposed to be due to the ability for a ground state vanadium atom to insert into propene molecules, which is not possible in the case of ethene.